

# Fundamentals of Electro-Thermo-Mechanical Reliability

India Semiconductor Mission Professional Development Course

Ganesh Subbarayan, James G. Dwyer Professor of Mechanical Engineering, Purdue University

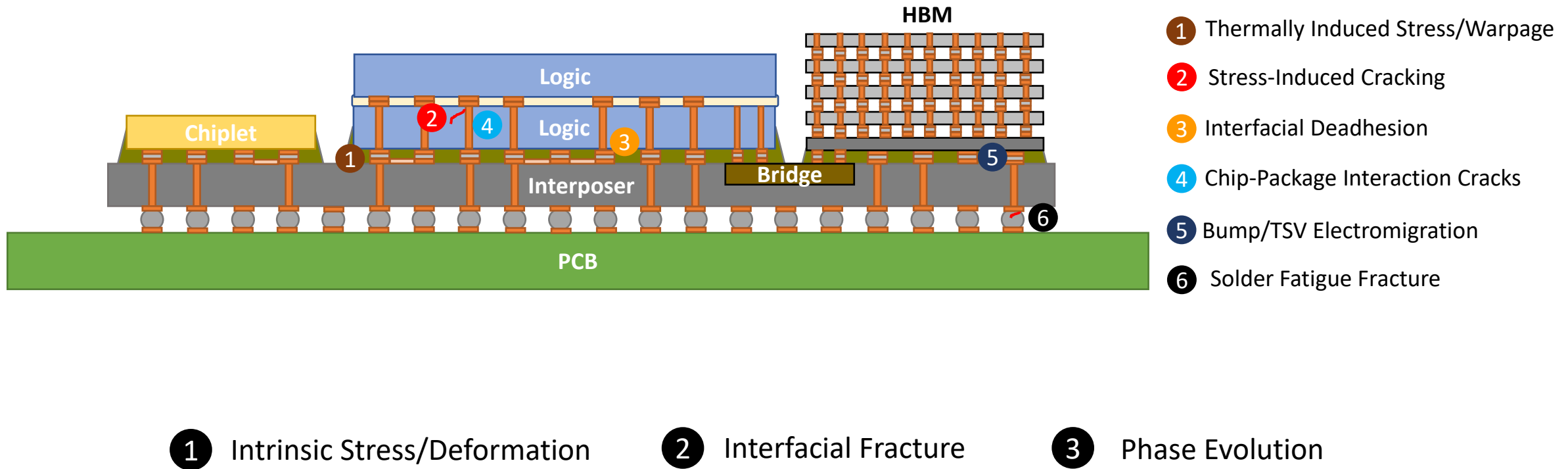
Director, Atalla Institute for Advanced System Integration and Packaging

Co-Director, SRC Center for Heterogeneous Integration Research in Packaging (CHIRP)

<https://engineering.purdue.edu/ASIP>, <https://engineering.purdue.edu/CHIRP>

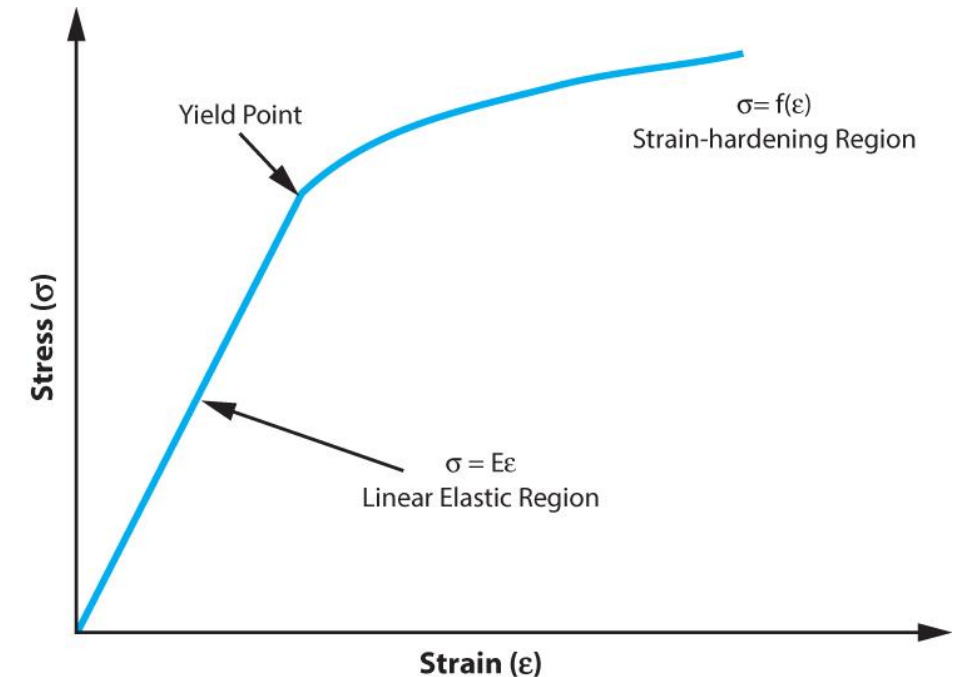
October 19, 2024

# General Reliability Concerns in Advanced Packaging

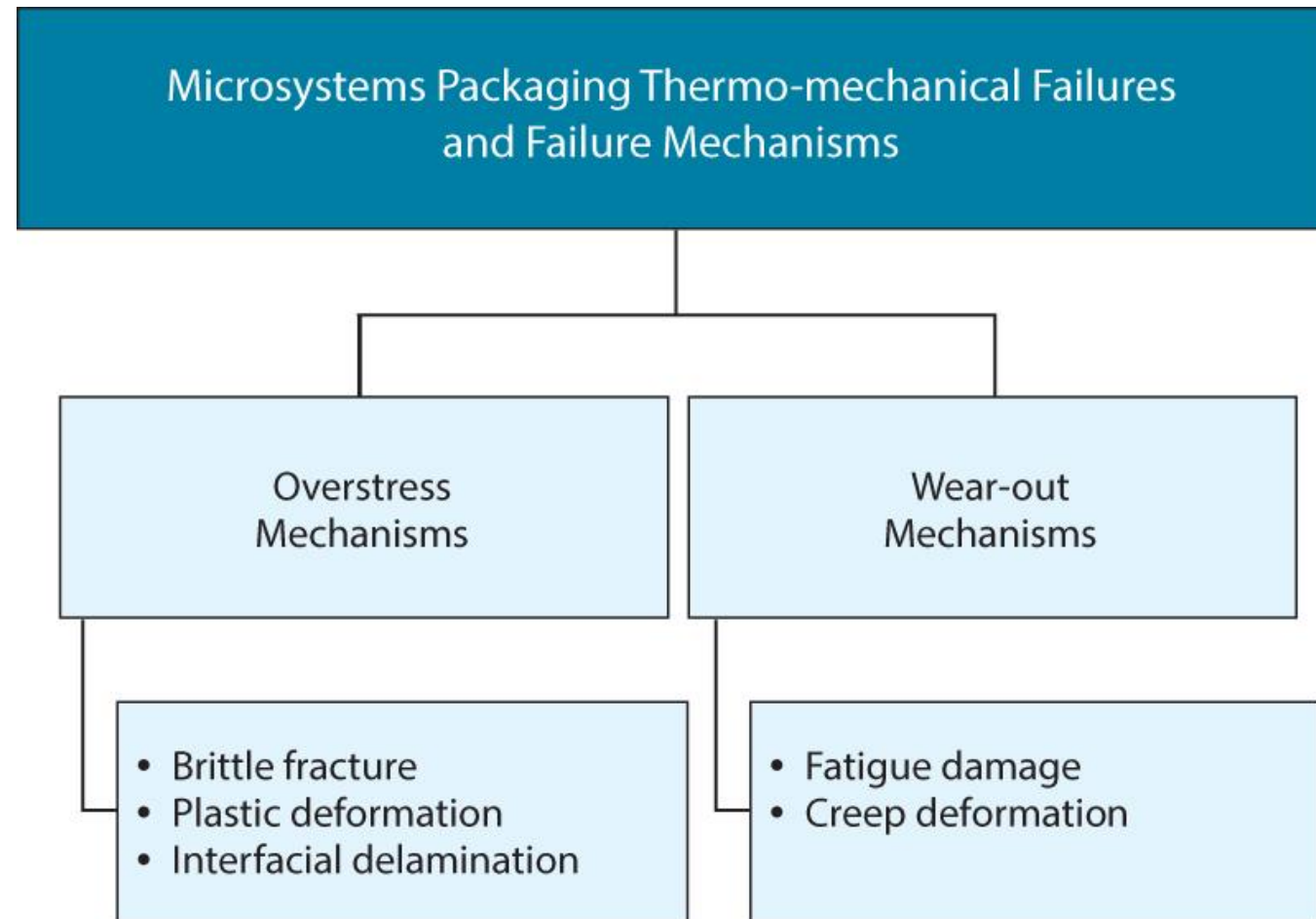


# Impact of Thermo-Mechanical Behavior

- Thermal Stress
  - Primary cause of many observed failures
- Package Deformation, Warpage
  - Loss of manufacturability, reduction of life
- Brittle Cracks (typically in the die)
  - Catastrophic failure during fabrication or use
- Interfacial de-adhesion (in thin films)
  - Catastrophic failure during fabrication or use
- Ductile Fatigue Cracks (typically in the solder joint)
  - Product life shorter than expected
- Electromigration in Circuit Lines and in Solder Joints
  - Product life shorter than expected
- Diffusion-Reaction (in solder joints)
  - Product life shorter than expected



# Failure Mechanisms in Microsystem Packages



# Effective Thermal Expansion of a Component

# Flip-Chip Package Analysis

- How to estimate deformation and stress in the die and the PCB?
  - Use bar approximation for each layer

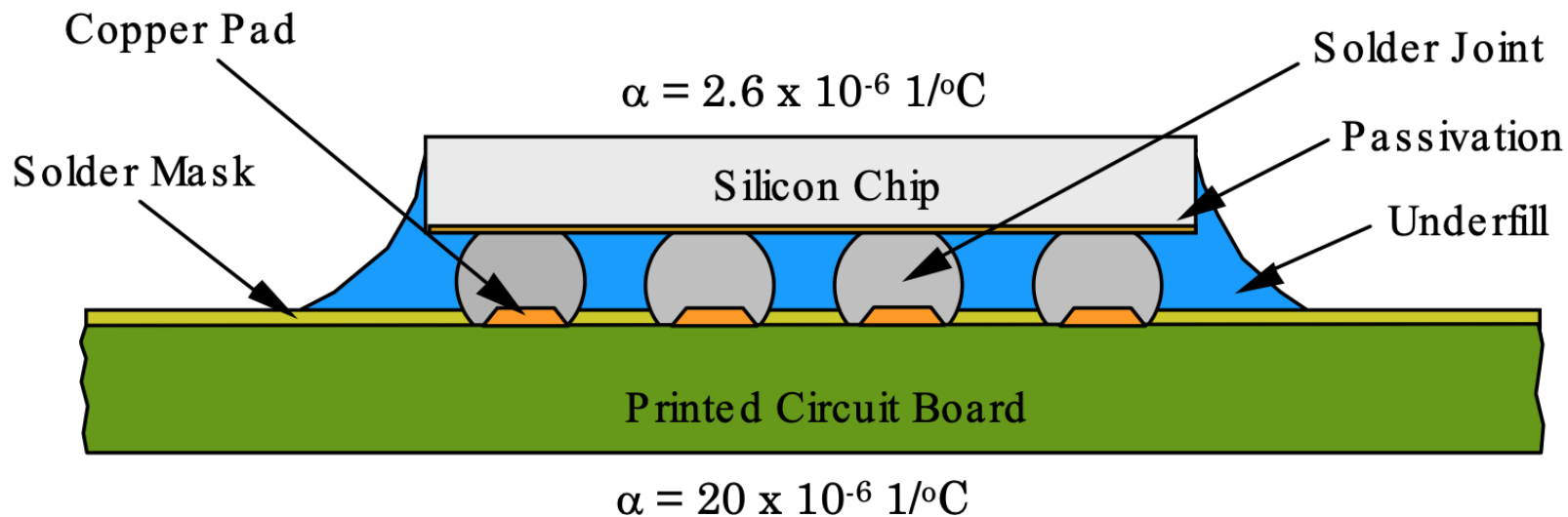
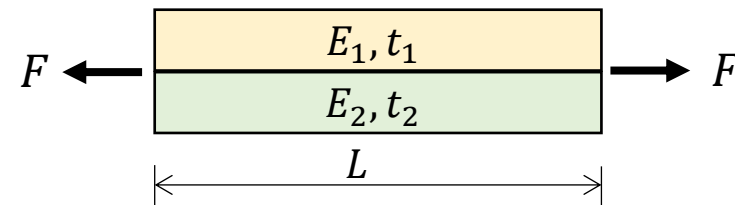


Image: Kaysar Rahim, M ; Suhling, J.C ; Jaeger, R.C ; Lall, P ; Knight, R ; Strickland, M ; Blanche, J  
Thermal and Thermomechanical Proceedings 10th Intersociety Conference on Phenomena in  
Electronics Systems, 2006. ITERM 2006, 2006, p.1379-1389

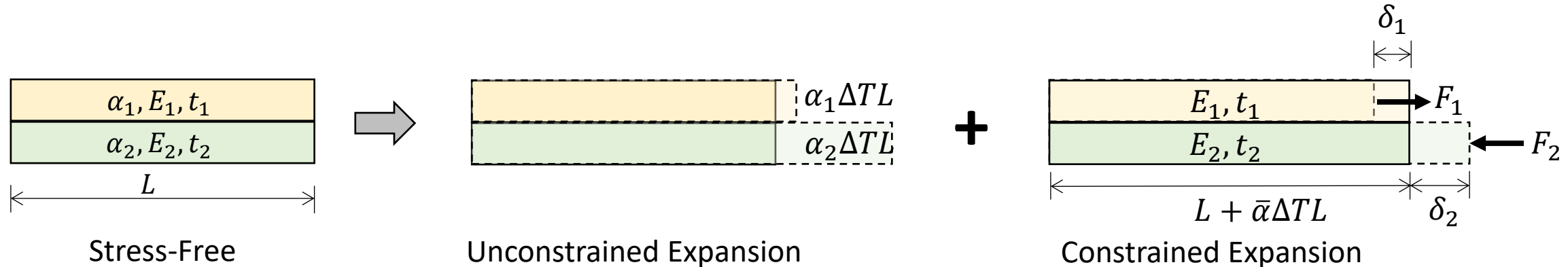
# Effective Elastic Modulus of a Bimaterial Bar

- Consider the bimaterial bar subject to force



- Equivalent to two springs in parallel, recall stiffness of each bar is  $k_i = \frac{E_i A_i}{L}$  ( $A_i = t_i w$ ,  $w$  = width/depth into the plane)
- Effective stiffness is  $\bar{k} = k_1 + k_2$  or  $\frac{\bar{E}(A_1+A_2)}{L} = \frac{E_1 A_1}{L} + \frac{E_2 A_2}{L}$
- Thus, effective elastic modulus is 
$$\boxed{\bar{E} = \frac{E_1 t_1 + E_2 t_2}{t_1 + t_2}}$$

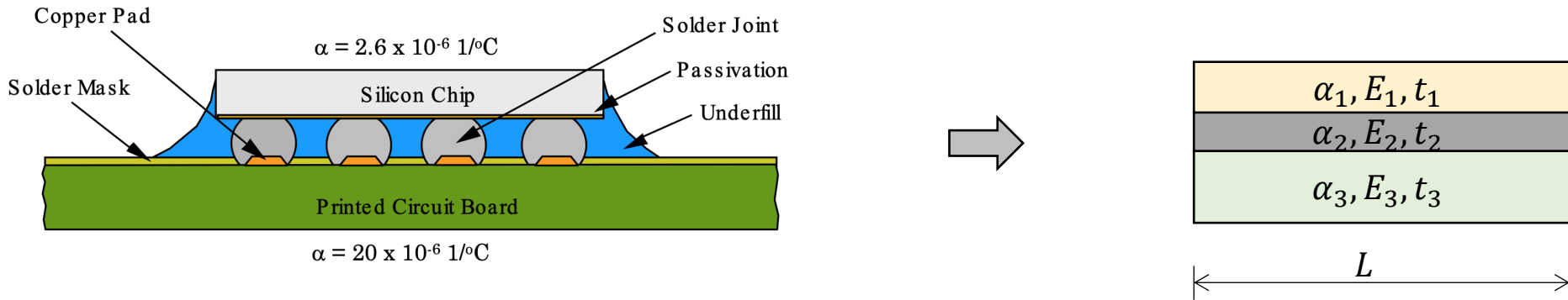
# Effective Coefficient of Thermal Expansion



- Compatibility Condition:  $L + \alpha_1 \Delta T L + \delta_1 = L + \alpha_2 \Delta T L - \delta_2$
- Force Balance:  $F_1 = F_2$
- Deformation of each layer (assuming bars):  $\delta_i = \frac{F_i}{k_i} = \frac{F_i}{(E_i A_i / L)}, A_i = t_i w, i = 1, 2$
- Solve to get the effective CTE of bimaterial bar:

$$\bar{\alpha} = \frac{\alpha_1 E_1 t_1 + \alpha_2 E_2 t_2}{E_1 t_1 + E_2 t_2}$$

# A Model for Multilayer Structures



- Generalize the earlier derivations for  $n$ -layer structure:

$$\bar{E} = \frac{\sum_{i=1}^n E_i t_i}{\sum_{i=1}^n t_i}, \quad \bar{\alpha} = \frac{\sum_{i=1}^n \alpha_i E_i t_i}{\sum_{i=1}^n E_i t_i}$$

- For middle layer, use volume weighted modulus and CTE:

$$E_2 = \frac{E_{sol}V_{sol} + E_{un}V_{un}}{V_{sol} + V_{un}}, \quad \alpha_2 = \frac{\alpha_{sol}V_{sol} + \alpha_{un}V_{un}}{V_{sol} + V_{un}}$$

- Expansion of the package as a whole:

$$\delta = \bar{\alpha} \Delta T L$$

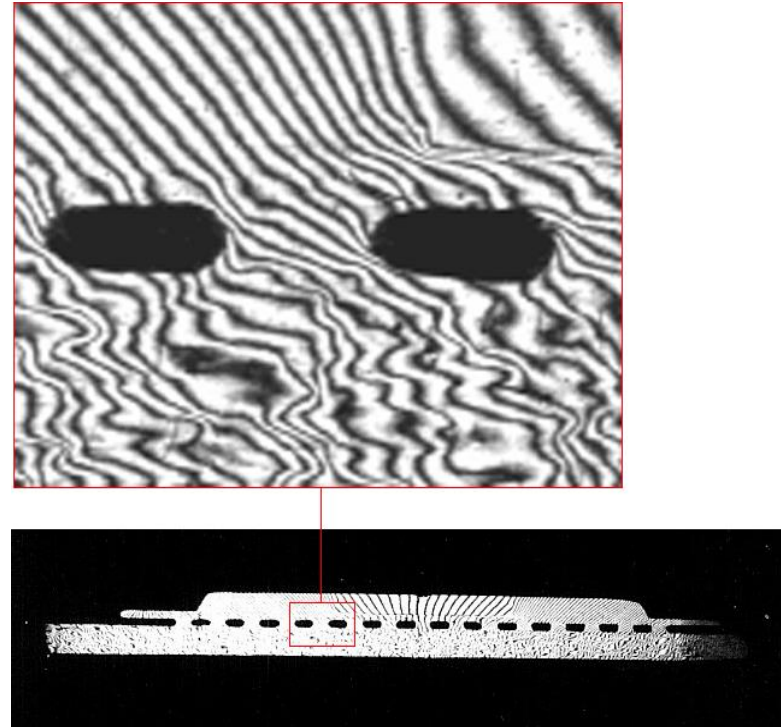
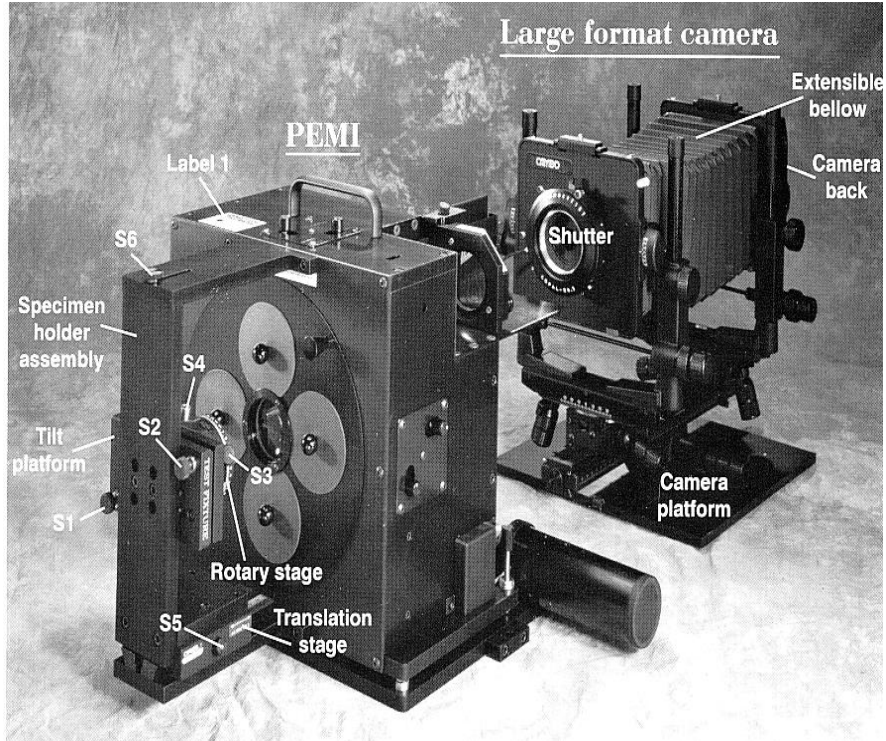
- Force in any layer:

$$F_i = k_i \delta_i = k_i (\delta - \alpha_i \Delta T L) = \frac{E_i A_i}{L} (\bar{\alpha} - \alpha_i) \Delta T L = E_i A_i (\bar{\alpha} - \alpha_i) \Delta T$$

- Stress in any layer:

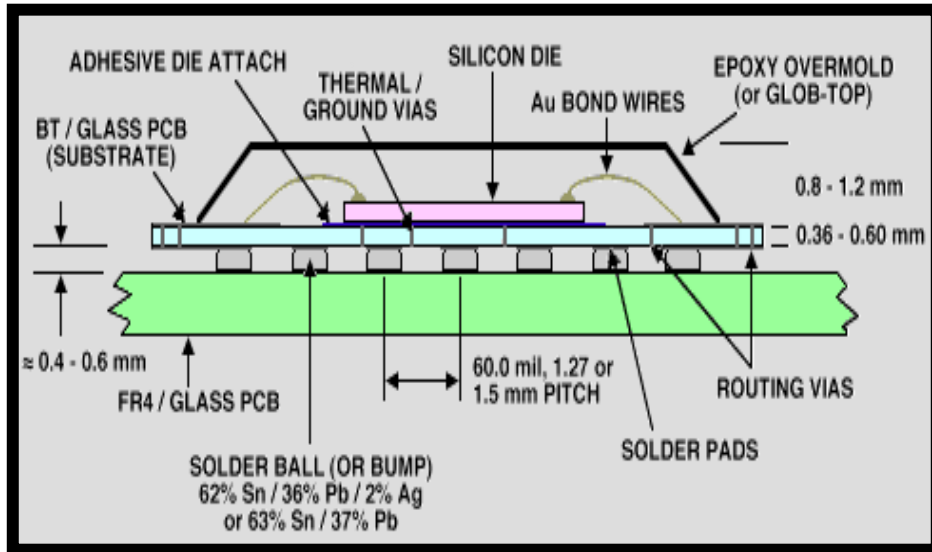
$$\sigma_i = \frac{F_i}{A_i} = E_i (\bar{\alpha} - \alpha_i) \Delta T$$

# Deformation in Electronic Packages

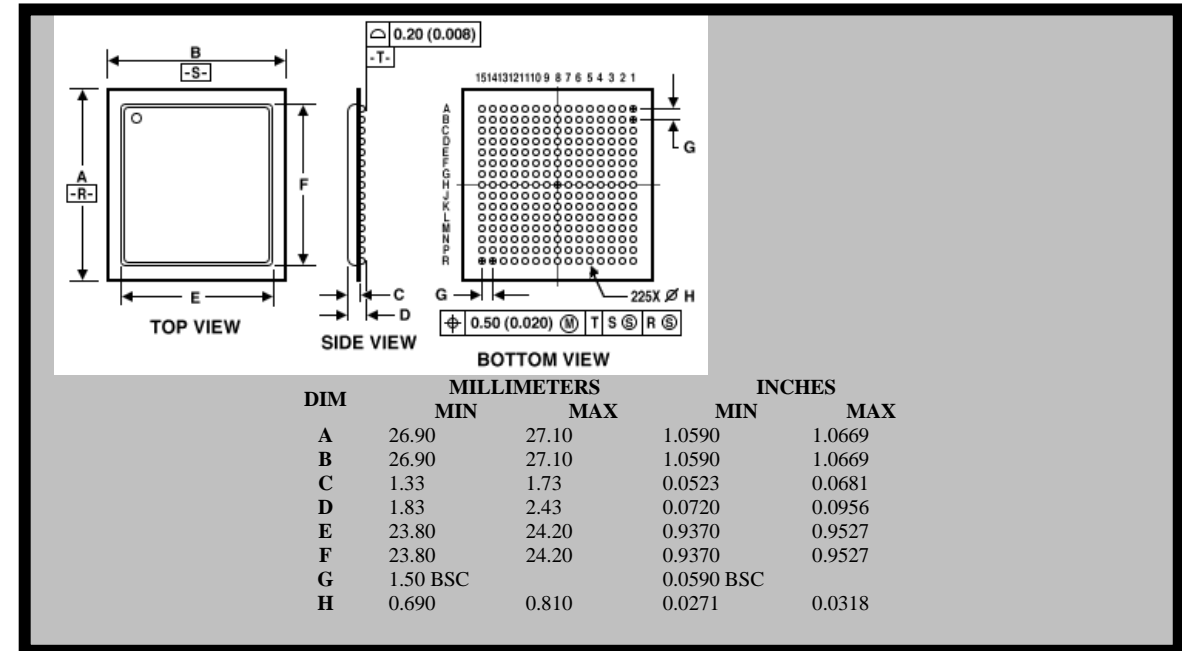


Left: Fringe Pattern Picture of Cross Section of 225 I/O PBGA  
Right: Personal Moiré Interferometer (PEMI) developed by IBM

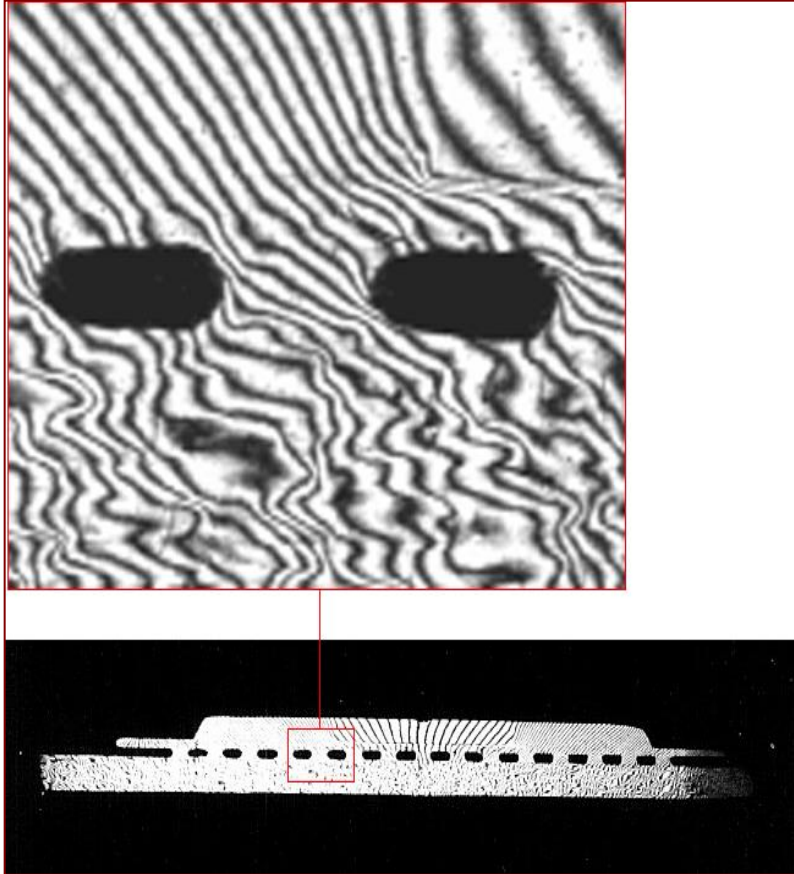
# Package Deformation Example



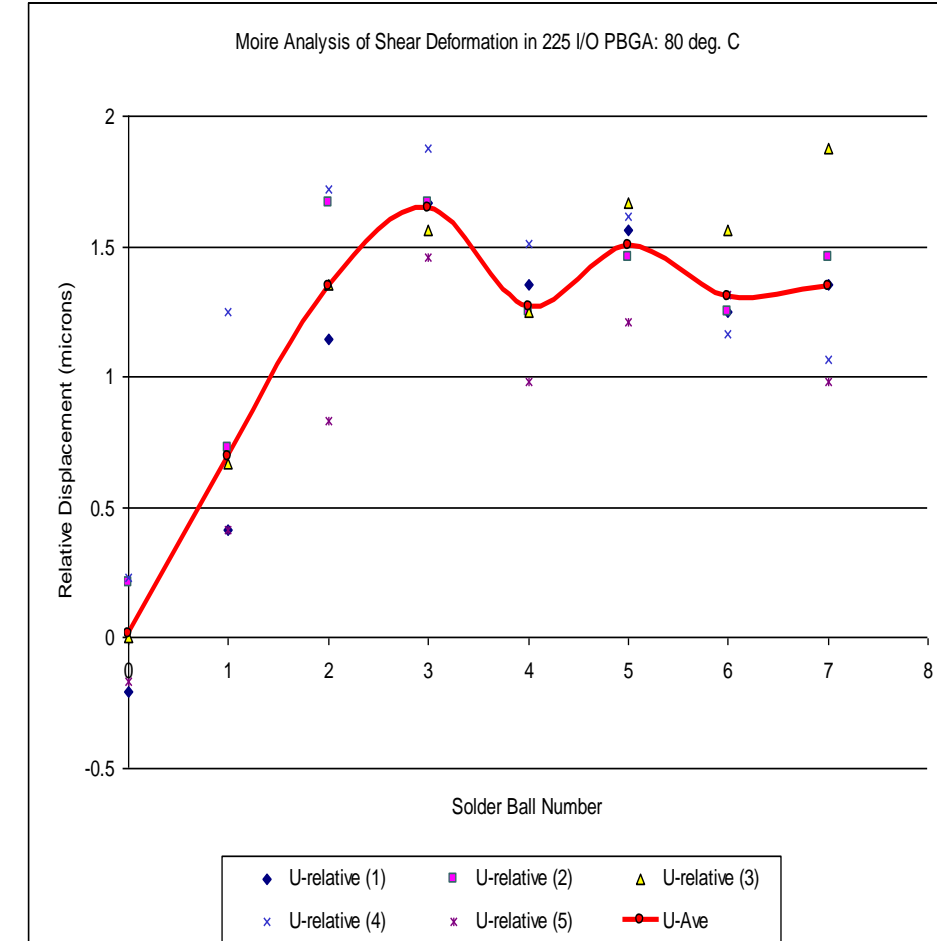
225 I/O Plastic Ball Grid Array (PBGA) Package



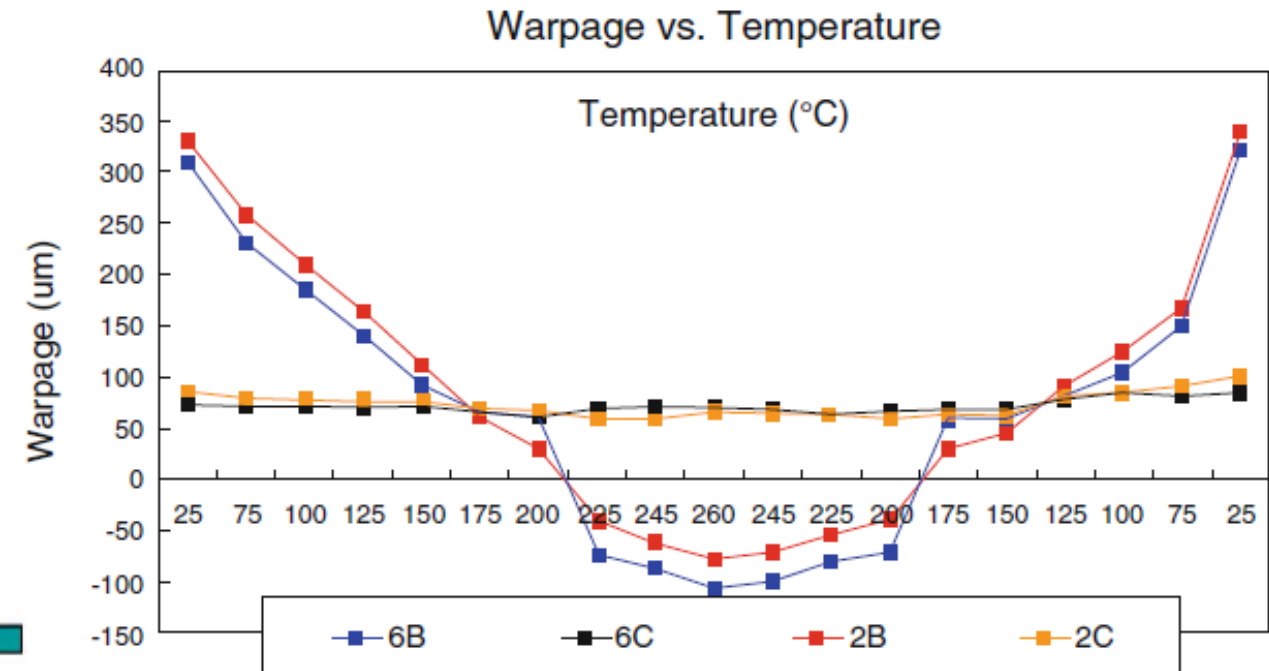
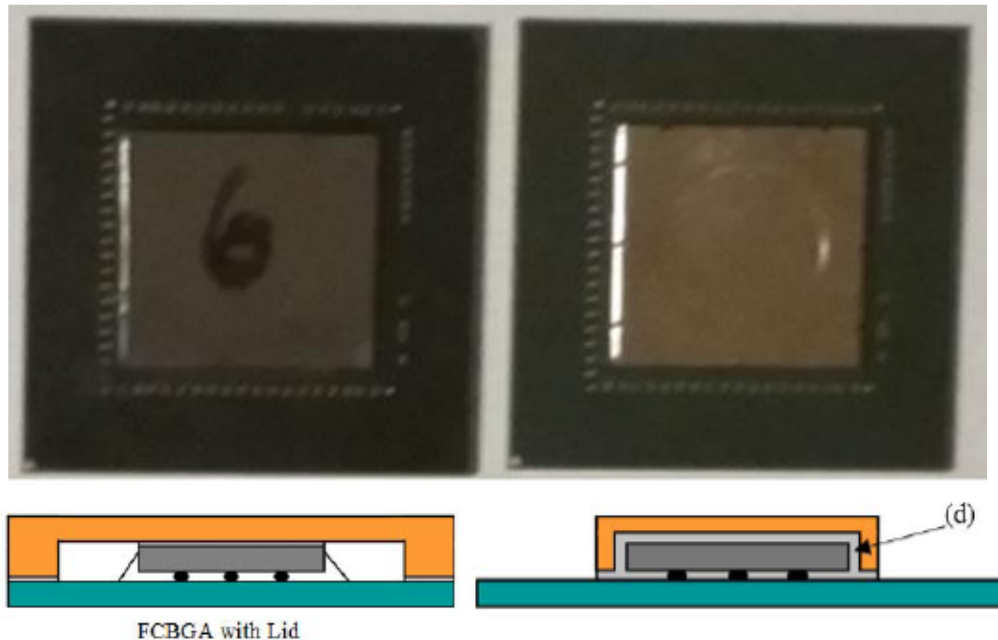
# Solder Joint Shear Deformation



225 I/O Plastic Ball Grid Array (PBGA) Package



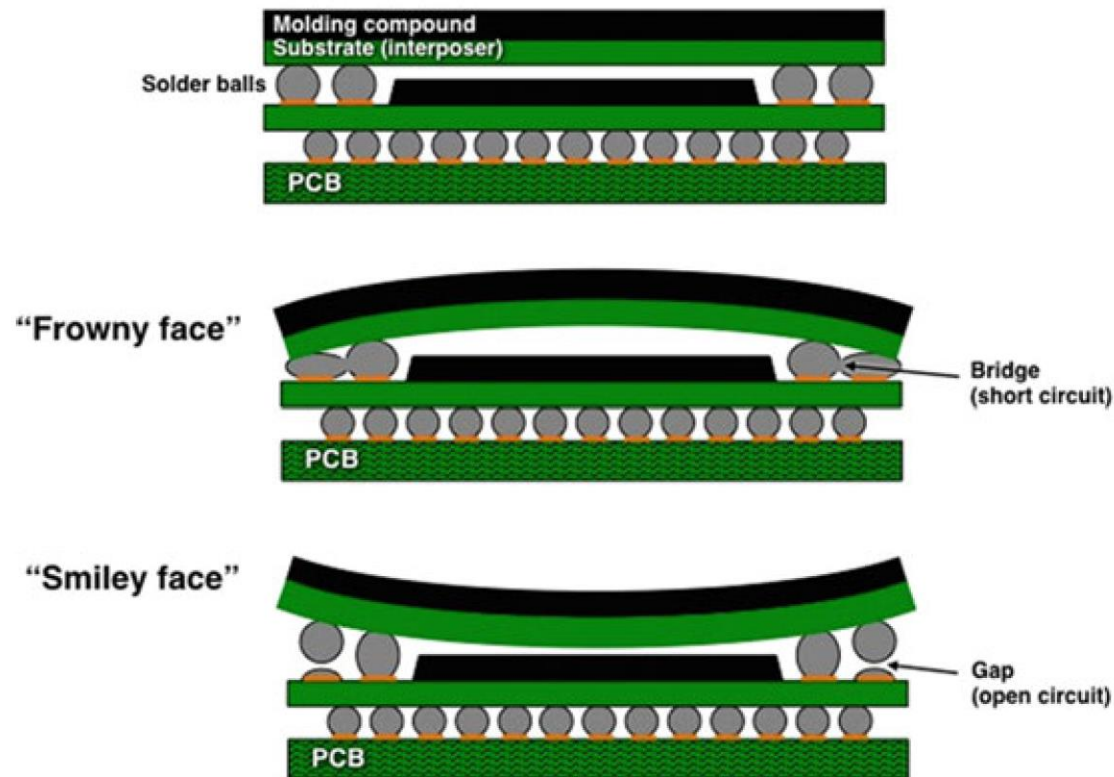
# Warpage in Flip-Chip Package



Shadow Moire' data for bare die and capped-die flip-chip packages (6B, 2B, 6C and 2C stand for package types)

Y. Shen, L. Zhang, W.H. Zhu, J. Zhou, X.J. Fan, IEEE Transactions on Components, Packaging and Manufacturing Technology, 2016

# Impact of Warpage

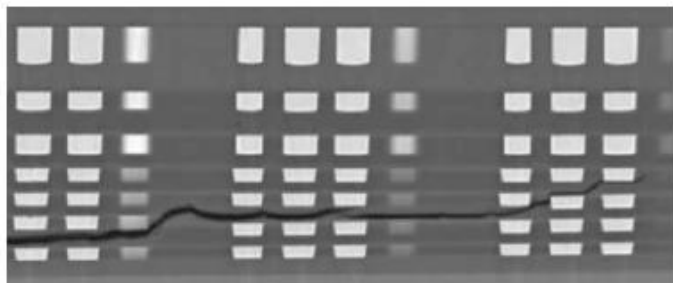
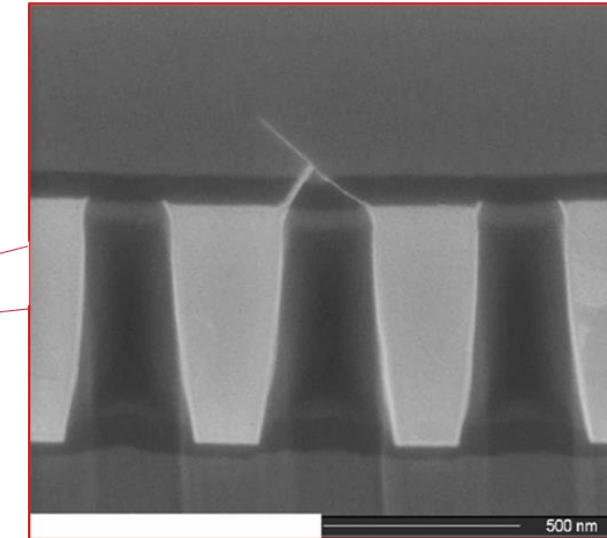
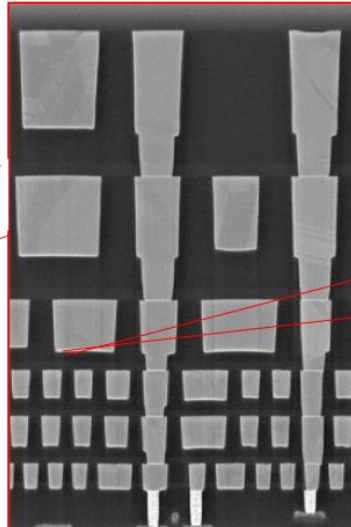
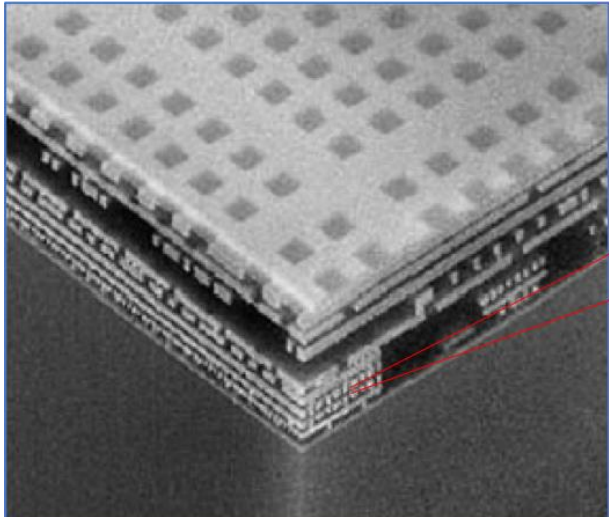


Vianco, 2017

# Brittle Fracture

# Die Cracking

- “Back-End-of-Line” (BEOL) contains re-entrant corners, multi-material junctions
- Cracks usually initiate from these locations



Zhang et al., 2008

T. Gupta, 2009  
G. B. Alers et al., IEEE TDMR, 2004

# Chip-Package “Interaction”

- Brittle chips fail under stress induced by package during fabrication or thermal cycling

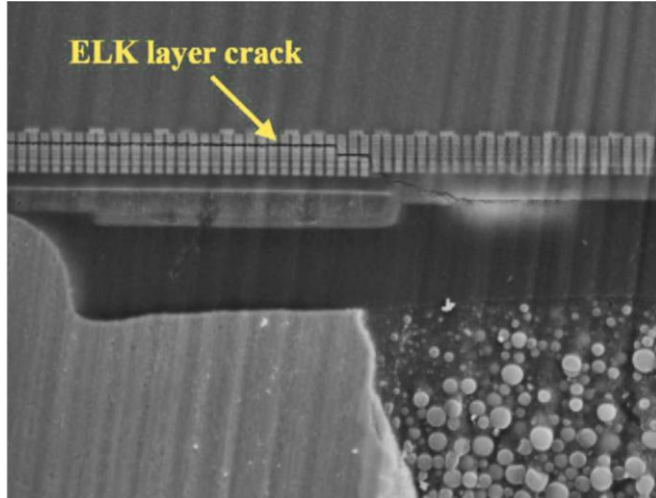


*Fig. 1: Dielectric cracking under a copper pillar bump*

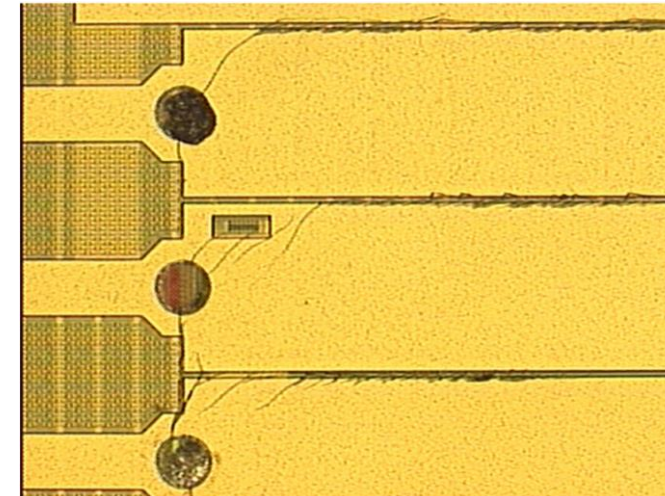


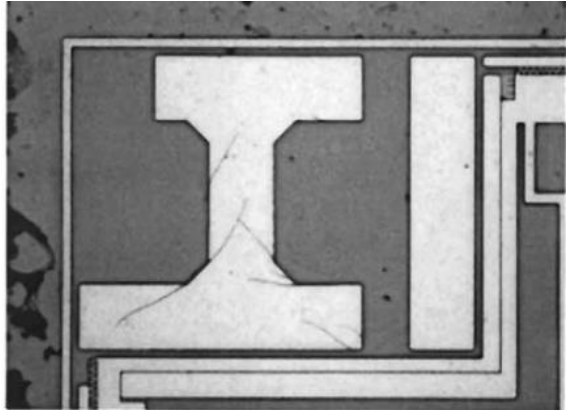
*Fig. 2: Passivation cracking over aluminum lines*

Chae et al, 2015

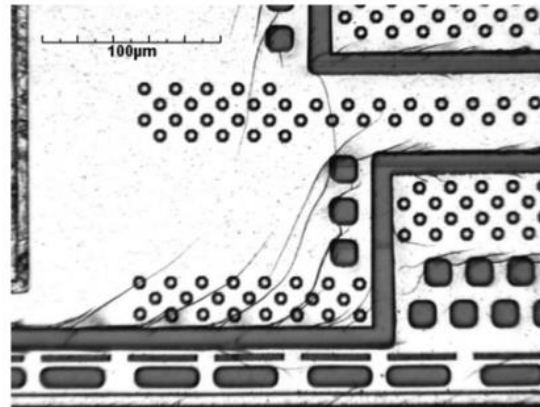
<https://www.electronicdesign.com/technologies/digital-ics/article/21800898/methodologies-to-mitigate-chippackage-interaction>

# More Passivation Film Cracking

## Examples of PO cracking

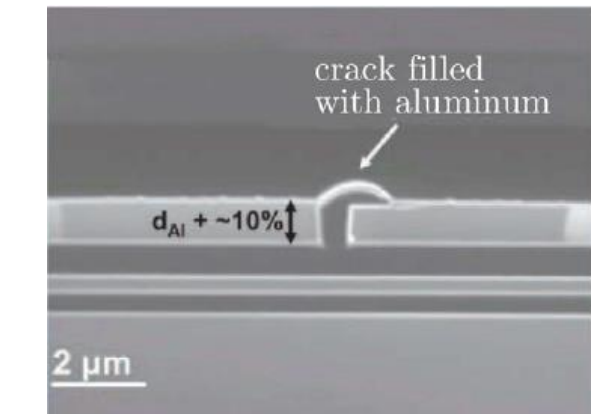
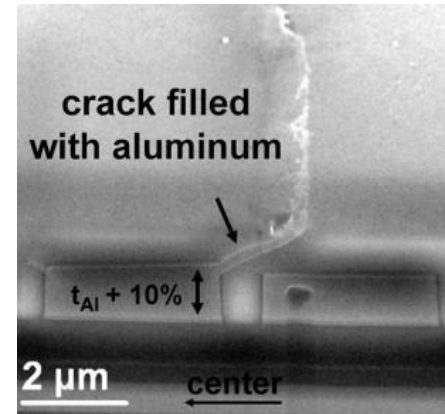


[\(Huang et al., JMPS, 2002\)](#)



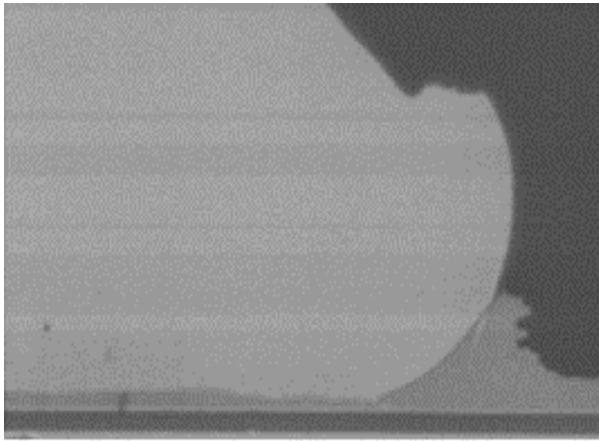
[\(Alpern et al., IEEE TDMR, 2009\)](#)

## Examples of Al extrusion

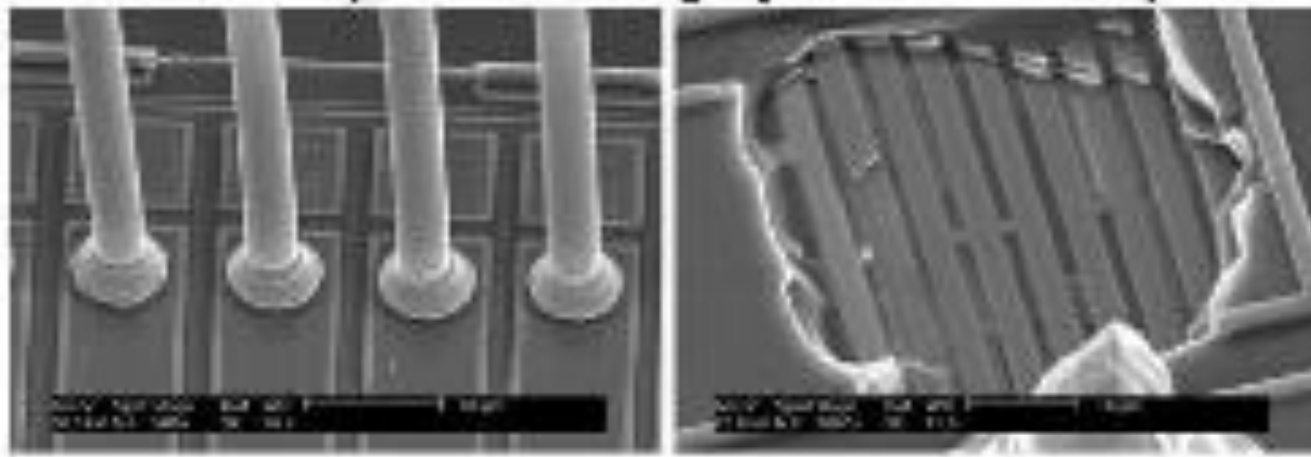
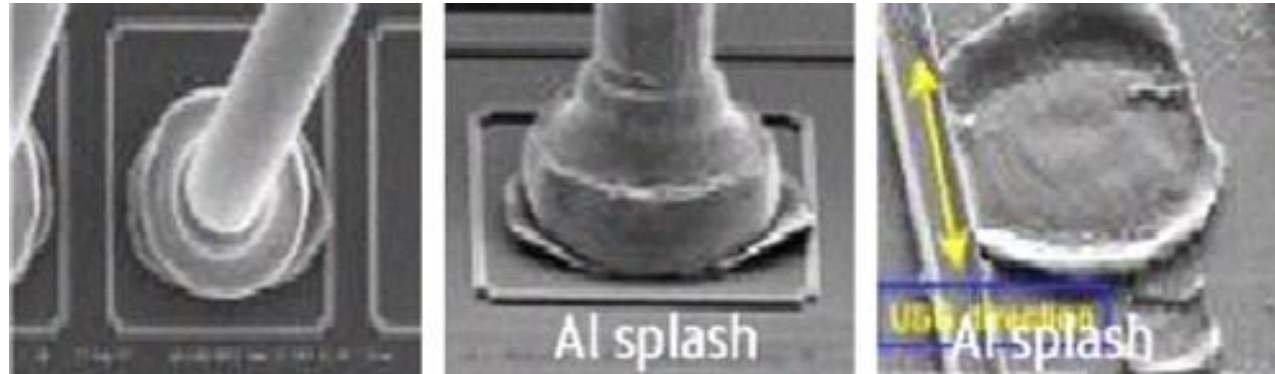


[\(Smorodin et al., IEEE , 2008\)](#)

# Wire Bond Reliability

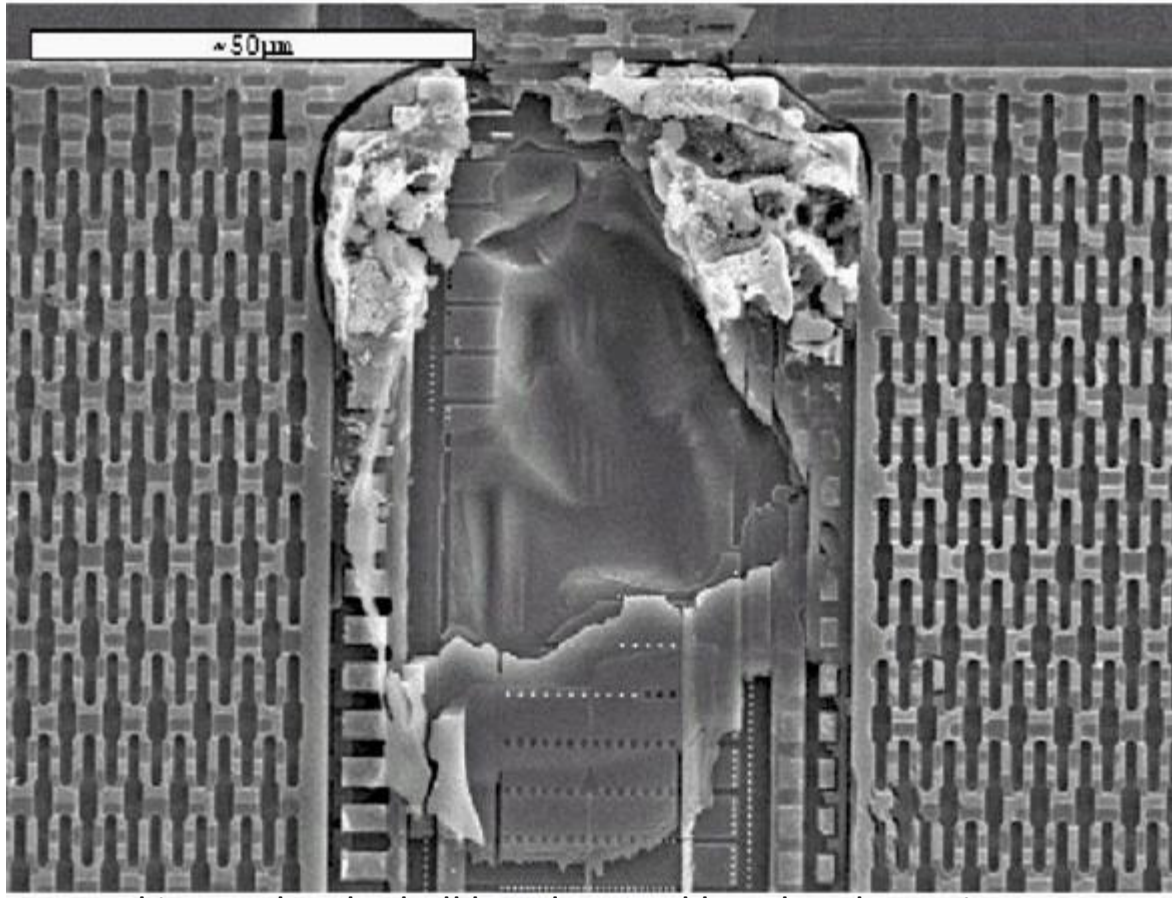


Hang et al., 2008



Wang et al., 2007

# Die Crack due to Wire Bond



ILD cracking under the ball bond caused bond pad catering

<https://www.electronicdesign.com/technologies/digital-ics/article/21800898/methodologies-to-mitigate-chippackage-interaction>

# Solder Ball Interface Failure: Drop Test

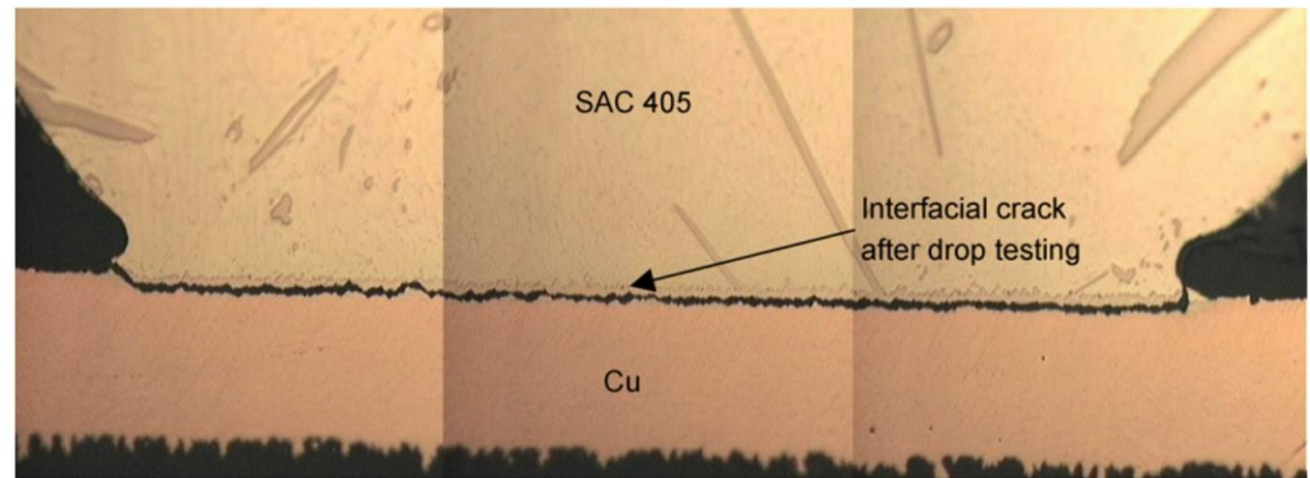
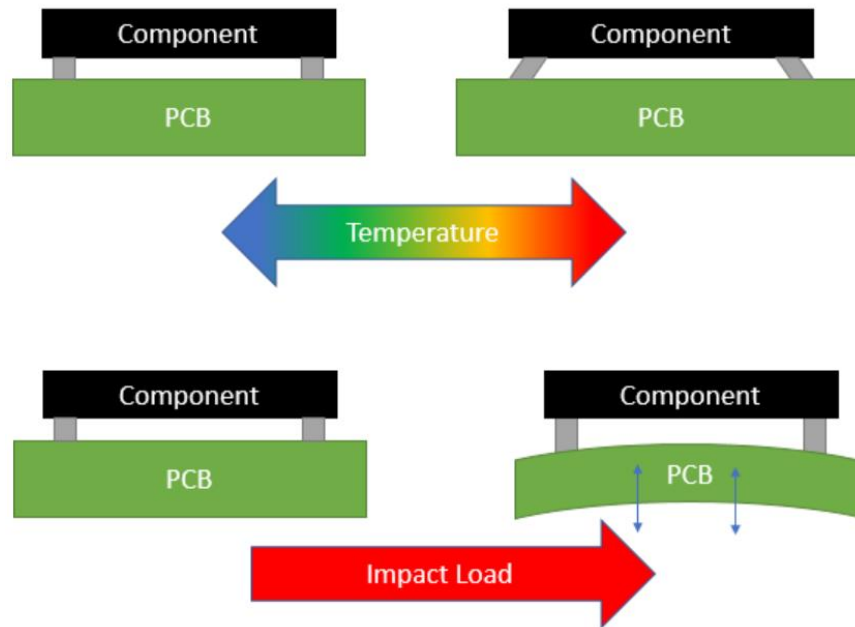
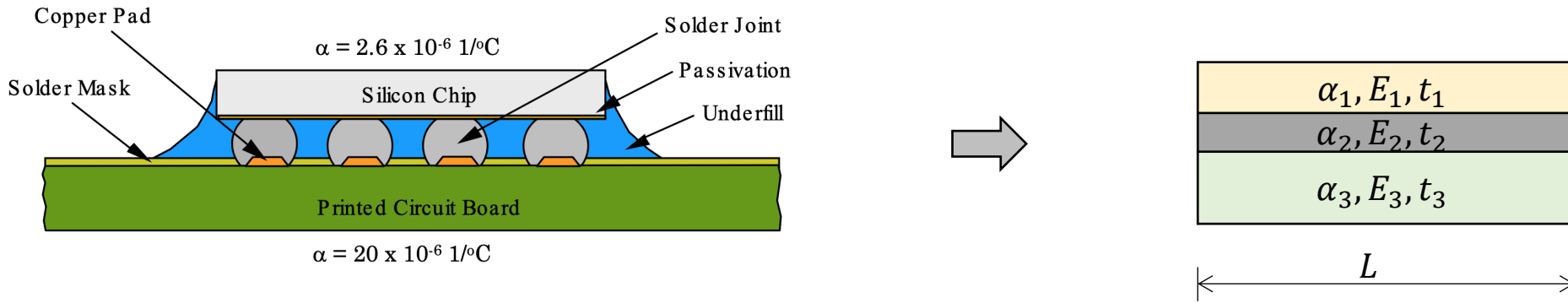


Figure 2(b) Brittle interfacial crack from high strain rate drop test on SAC405 solder on a Cu substrate with an ENIG surface finish (Suh 07)

# Brittle Fracture Case Study: Chip-Package Interaction

# Recap: One-Dimensional Model for Stress



- Generalize the earlier derivations for  $n$ -layer structure:

$$\bar{E} = \frac{\sum_{i=1}^n E_i t_i}{\sum_{i=1}^n t_i}, \quad \bar{\alpha} = \frac{\sum_{i=1}^n \alpha_i E_i t_i}{\sum_{i=1}^n E_i t_i}$$

- Stress in any layer:

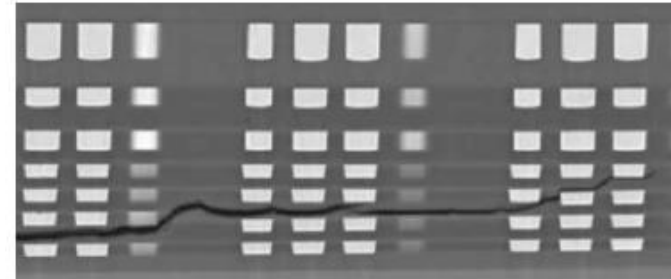
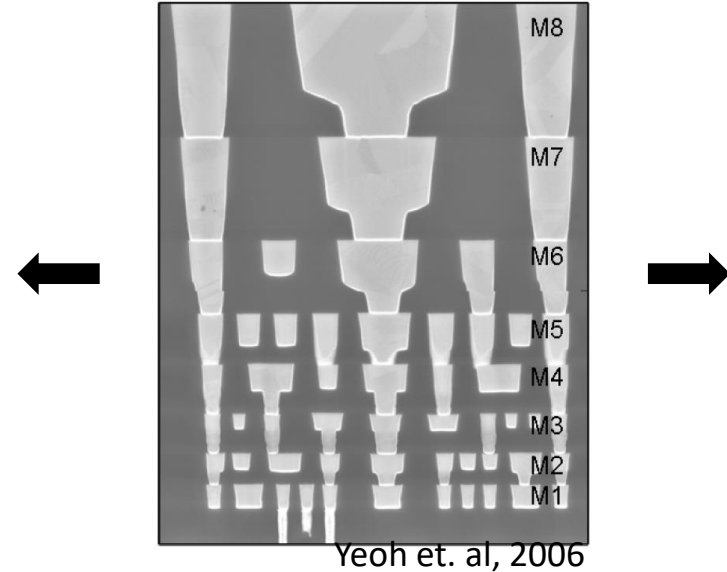
$$\sigma_i = \frac{F_i}{A_i} = E_i(\bar{\alpha} - \alpha_i)\Delta T$$

- Only captures average behavior not local stresses!

# Chip-Package Interaction (BEOL Fractures)

- BEOL structure has sharp corners
  - Singular stress at the material junctions

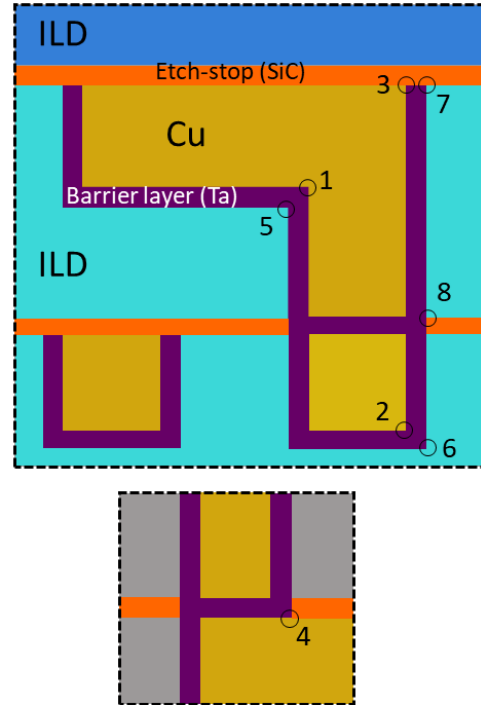
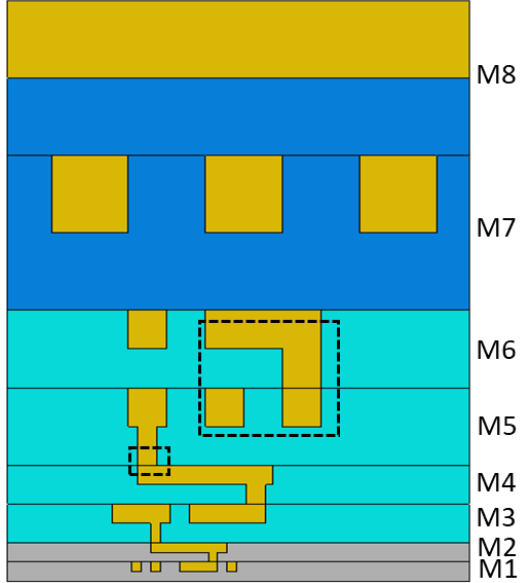
$$\sigma_{ij} = \sum_{n=1}^N K_n \frac{1}{r_{\lambda_n}} f_{ijn}(\theta) + \sigma_{ij0}(\theta)$$



Zhang et al., 2008

Y. Luo and G. Subbarayan, "A Study of Multiple Singularities in Multi-Material Wedges and their Use in Analysis of Microelectronic Interconnect Structures," Engineering Fracture Mechanics 74 (3) (2007) 416-430.

# Strength of Singularity – Risk of Crack Initiation

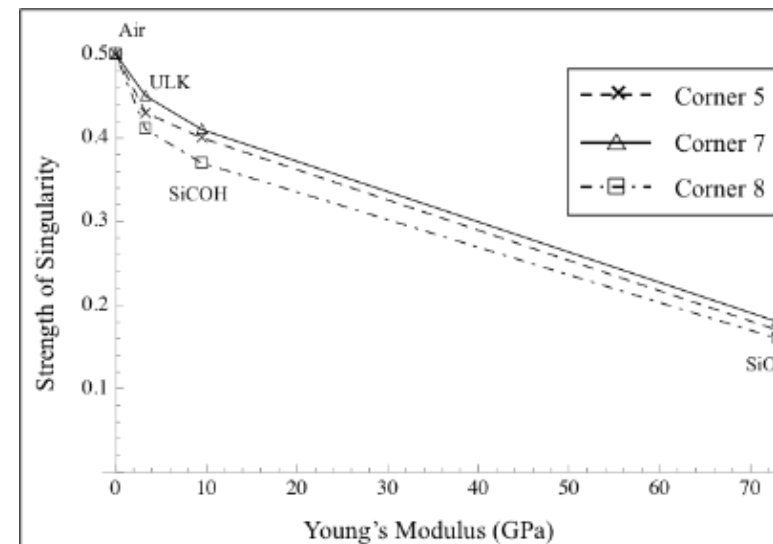


A. Tambat, H-Y. Lin, G. Subbarayan, D-Y. Jung, and B.G. Sammakia. "Simulations of Crack Initiation and Propagation in Inter-Layer Dielectrics Stacks: Understanding Assembly Induced Fracture in Dies" *IEEE Transactions on Device and Materials Reliability*, 12(2), 241-254 2012.

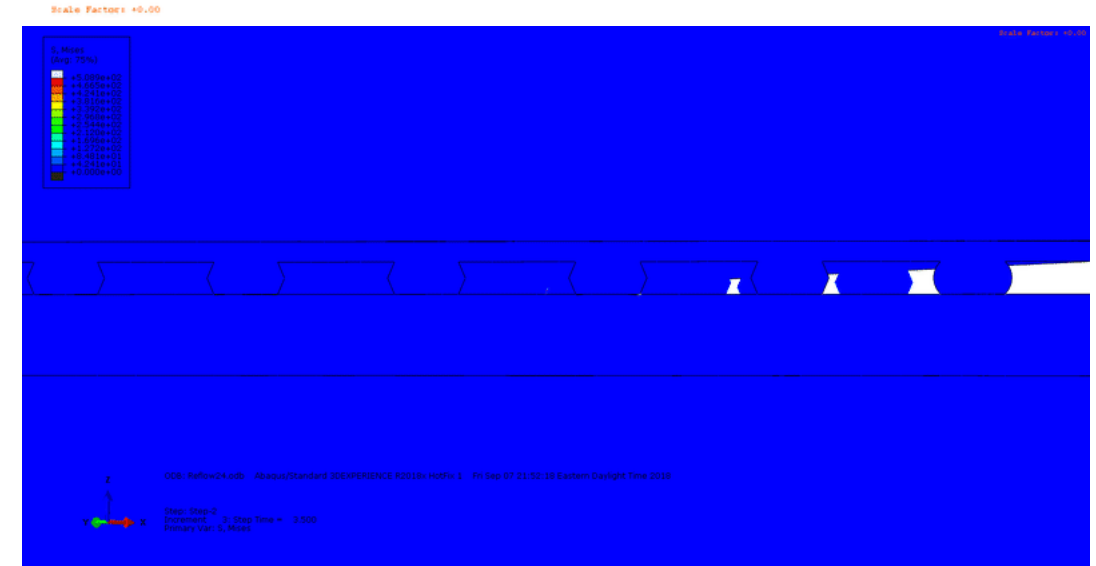
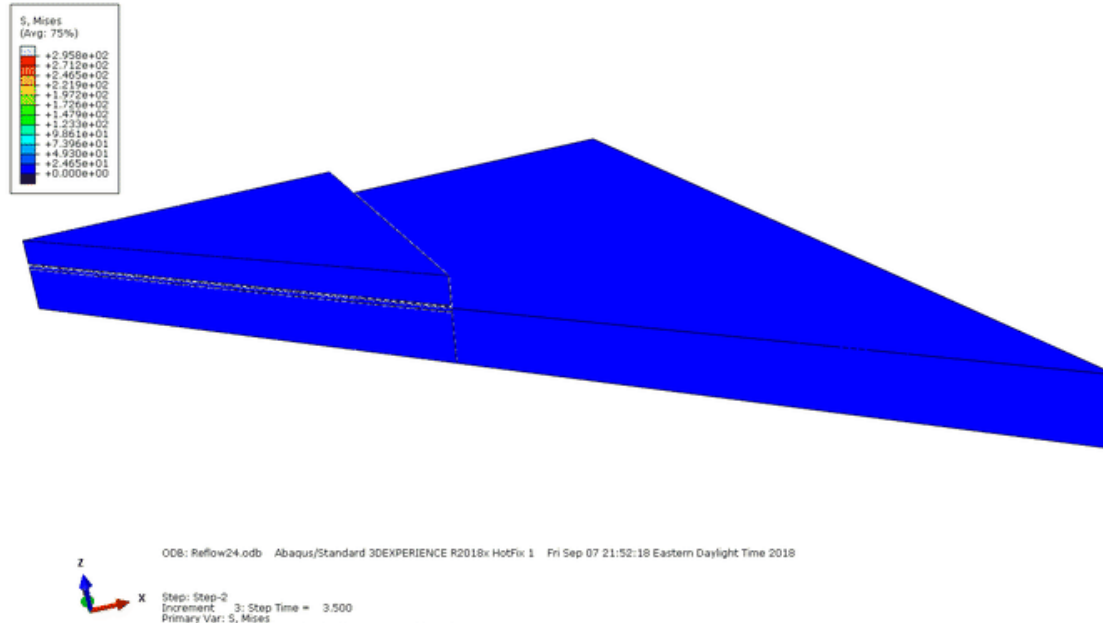
Site	Material Junction	Strength of Dominant Singularity	Strength of Second Singularity
5	Ta	0.17	0.02
		0.40	0.08
		0.43	0.09
7	SIC	0.18	0.02
		0.41	0.07
		<b>0.45</b>	0.08
8	Ta	0.16	0.03
		0.37	0.09
		0.41	0.10

ILD Materials

SiO <sub>2</sub>
SiCOH
ULK



# BEOL Stress Due to Chip-Package Interaction



A. Tambat, H-Y. Lin, G. Subbarayan, D-Y. Jung, and B.G. Sammakia. "Simulations of Crack Initiation and Propagation in Inter-Layer Dielectrics Stacks: Understanding Assembly Induced Fracture in Dies" *IEEE Transactions on Device and Materials Reliability*, 12(2), 241-254 2012.

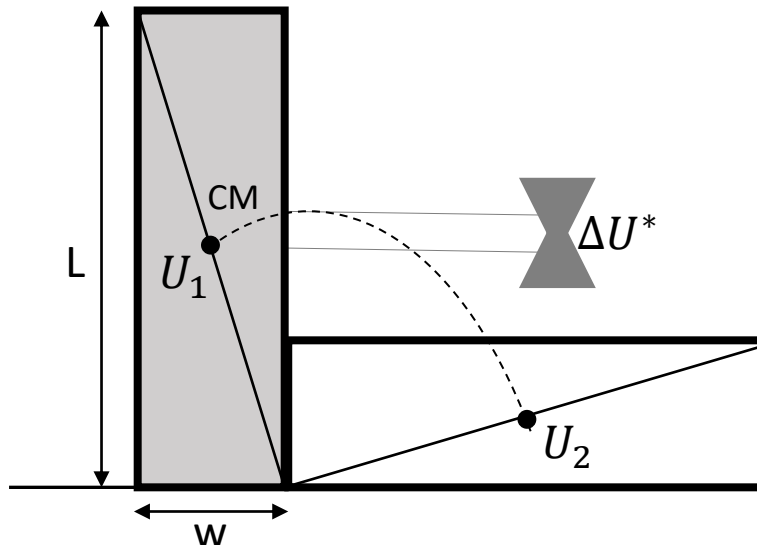
# Creep and Fatigue

# Introduction

- Degradation fundamental to all physical systems
  - Consequence of 2<sup>nd</sup> law of thermodynamics
  - Disorder (entropy) will tend to increase with time
- Mechanisms include creep, fatigue, oxidation, corrosion, wear, electromigration, stressmigration, dielectric breakdown...

# Degradation – Metastable States

- Materials/devices are typically in (thermodynamic) metastable states
- Consider the example of a vertical block
  - Can reach a lower potential energy state if pushed



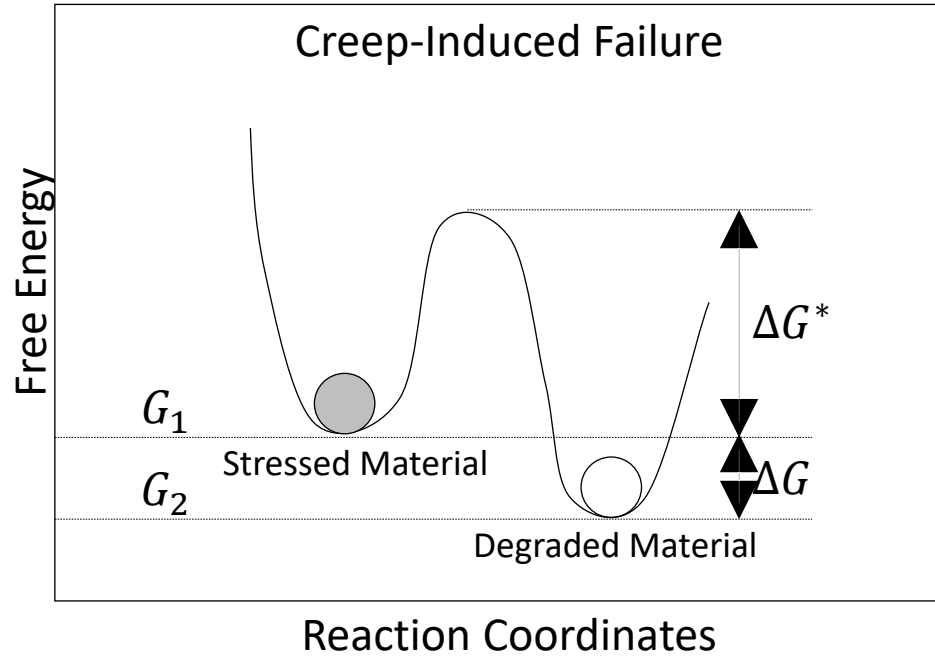
$$\Delta U = U_2 - U_1 = -mg \left( \frac{L - W}{2} \right)$$

$$\Delta U^* = mg \left( \frac{\sqrt{L^2 + W^2} - L}{2} \right)$$

Source: J.W. McPherson, Reliability Physics and Engineering:  
Time to Failure Modeling, 2<sup>nd</sup> Edition, Springer, 2013.

# Creep-Induced Failures

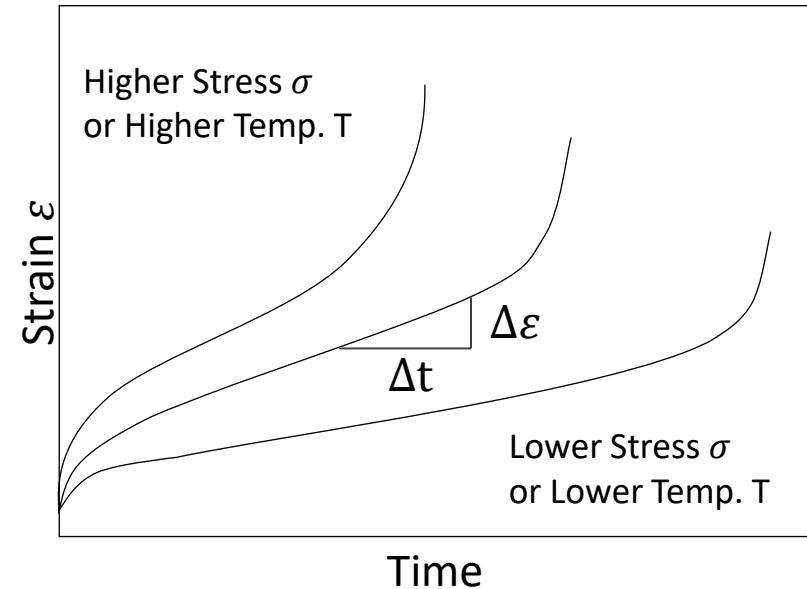
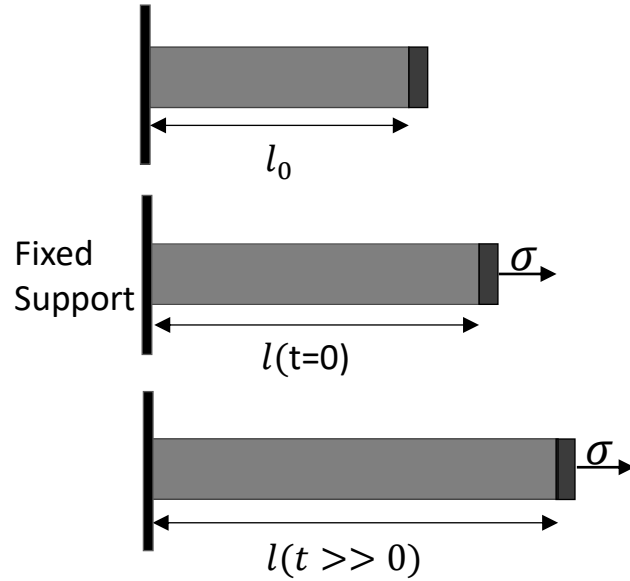
- Increase in strain with time at a constant stress
  - Can also lead to reduction/relaxation in stress for a fixed strain
- Leads to material degradation



When a mechanical stress is applied to a material, the material can become metastable with a driving force ( $\Delta G$ ) favoring the degraded state. However, the rate of the degradation (creep) is limited by the activation energy ( $\Delta G^*$ ) which is generally associated with dislocation movement along the slip planes

Source: J.W. McPherson, Reliability Physics and Engineering: Time to Failure Modeling, 2<sup>nd</sup> Edition, Springer, 2013.

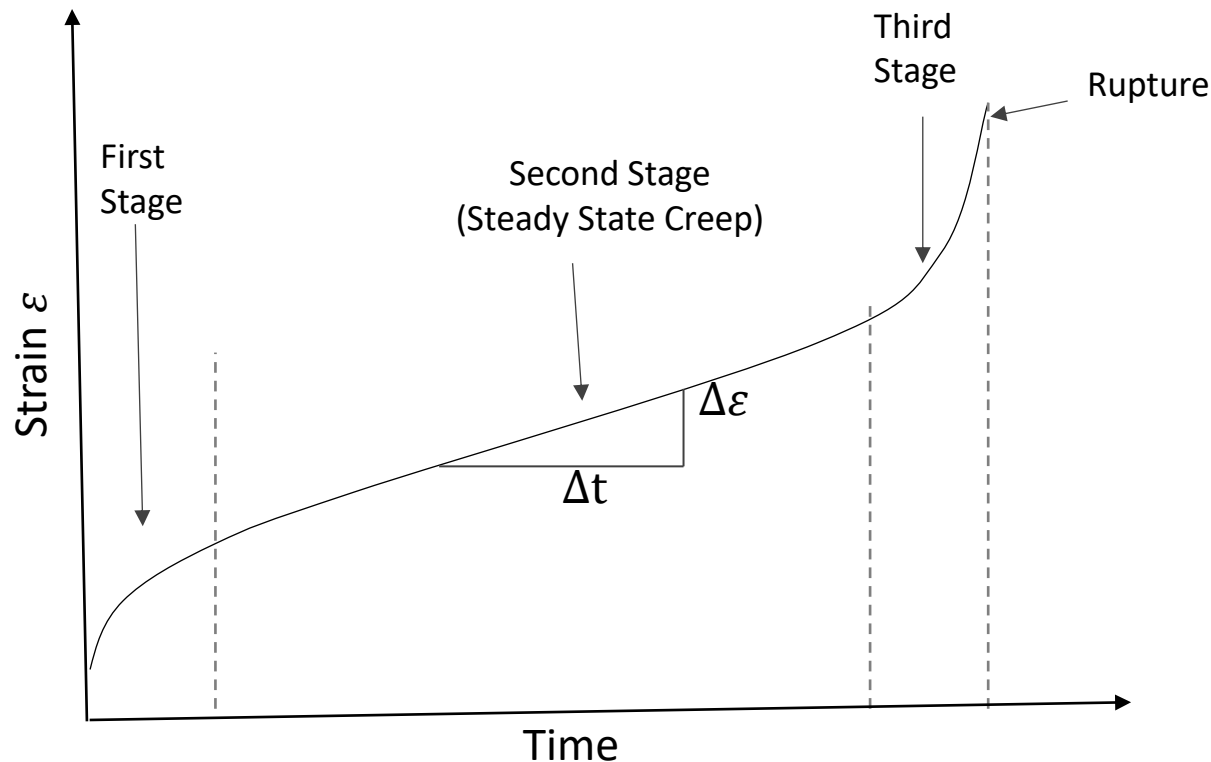
# Creep Response



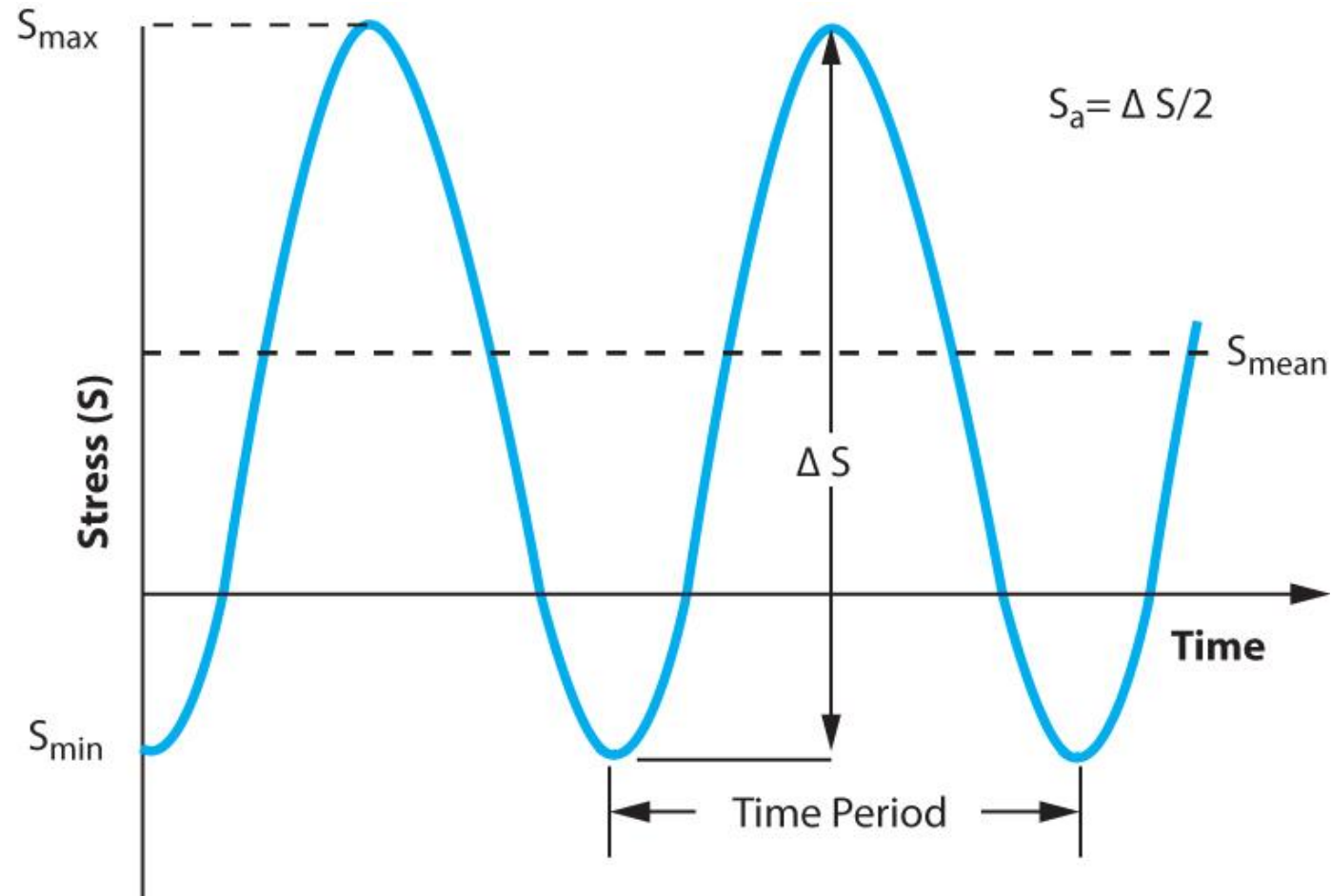
$$\varepsilon(t) = \frac{[l(t) - l_0]}{l_0}$$

Creep is likely when operating temperature  $T > 0.3 T_{melting}$  (absolute temperature in K)

# Creep Regimes



## Typical fatigue load cycle



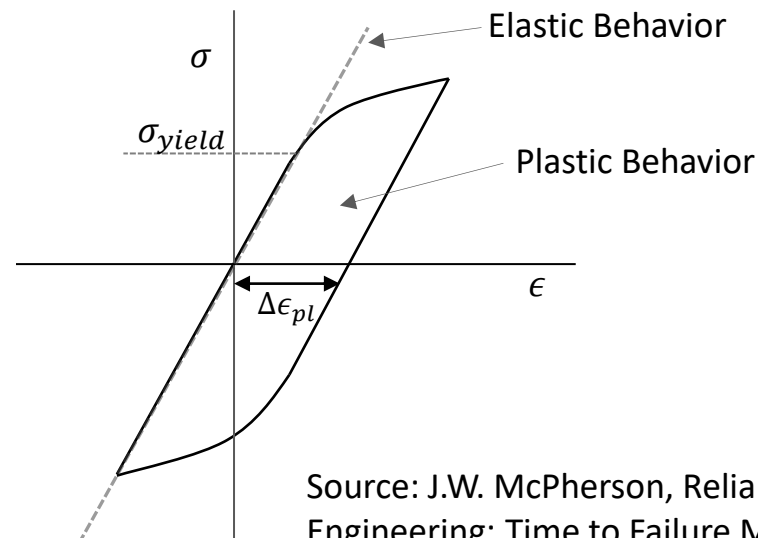
# Low-Cycle Fatigue

- Dominated by plastic deformation

Stress( $\sigma$ )–Strain( $\epsilon$ ) curve for one cycle of cyclical stress with  $\sigma_{mean} = 0$ .

Material damage/degradation can be expected during plastic deformation.

The amount of strain in the plastic region is represented by  $\Delta\epsilon_{pl}$



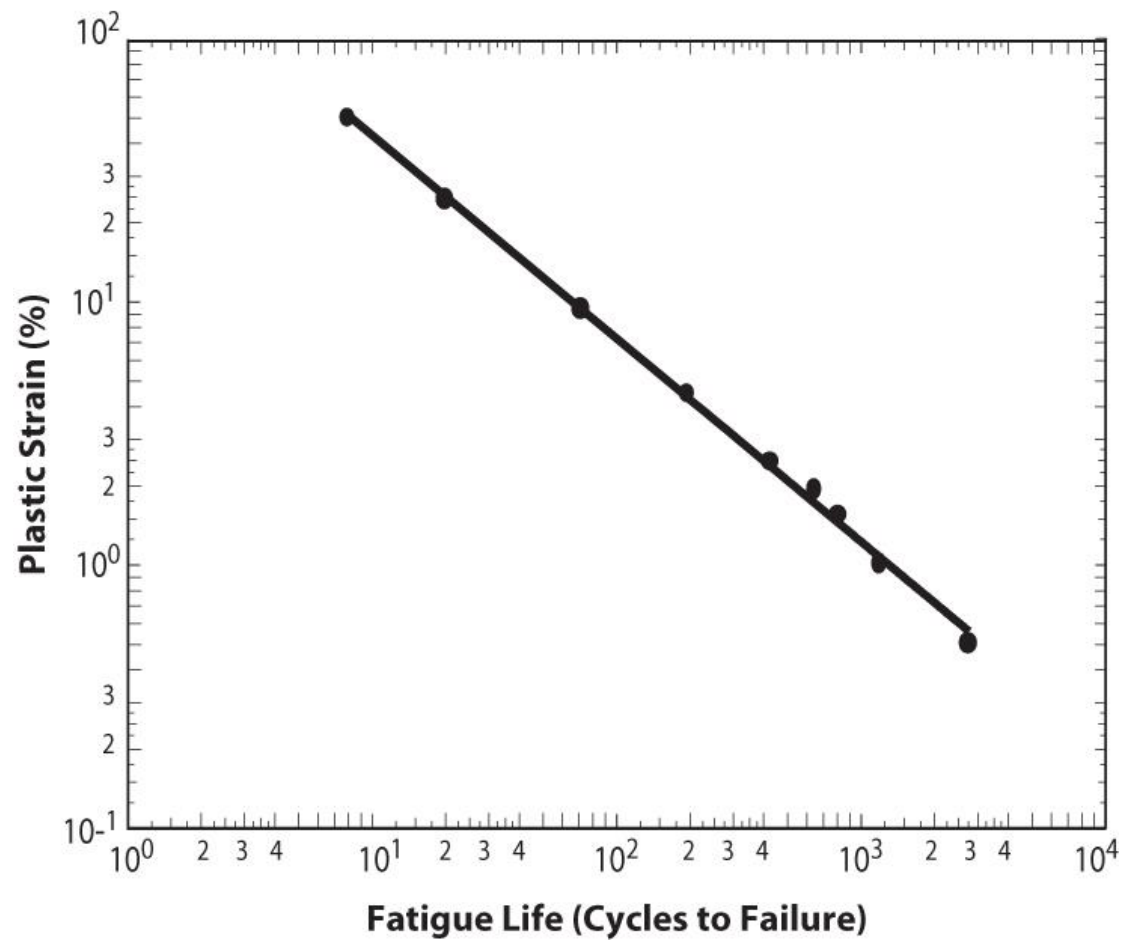
Source: J.W. McPherson, Reliability Physics and Engineering: Time to Failure Modeling, 2<sup>nd</sup> Edition, Springer, 2013.

- Damage accumulates until CTF=Cycles to failure

$$CTF = B_0 (\Delta\epsilon_{pl})^{-n}$$

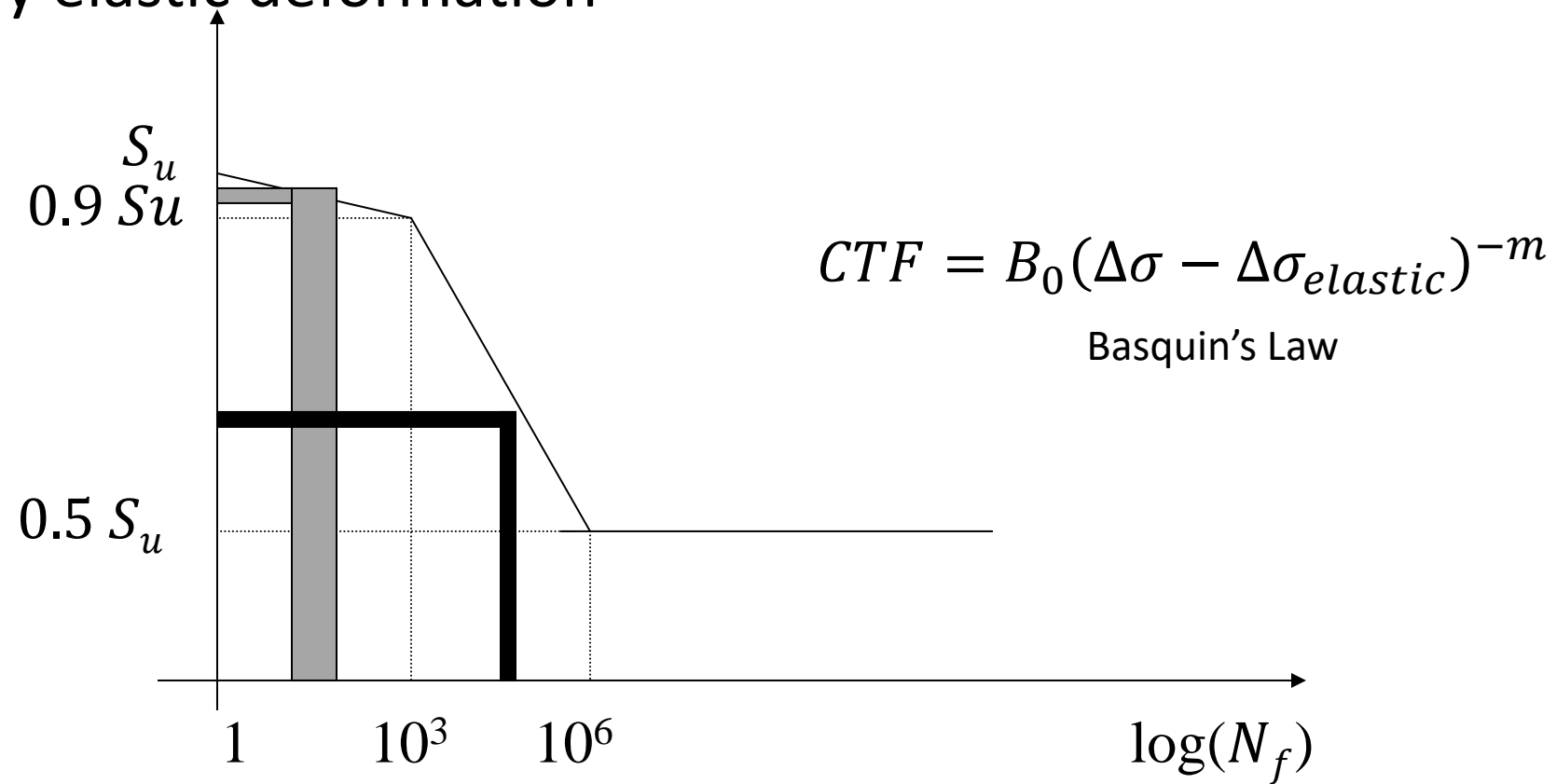
Coffin-Manson Law

## Effect of plastic strain on fatigue life

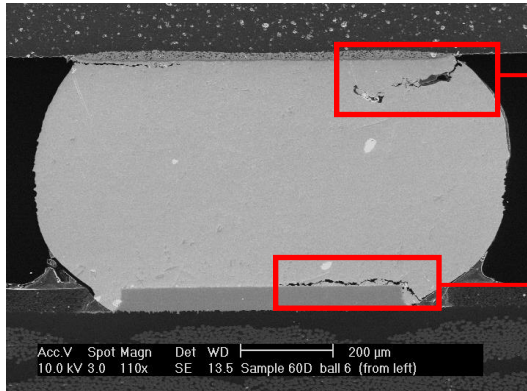


# High-Cycle Fatigue

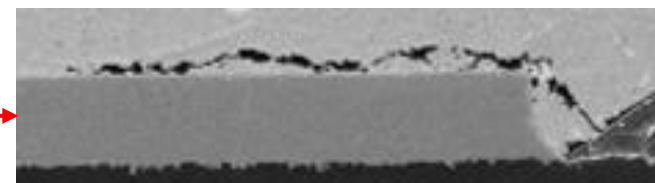
Dominated by elastic deformation



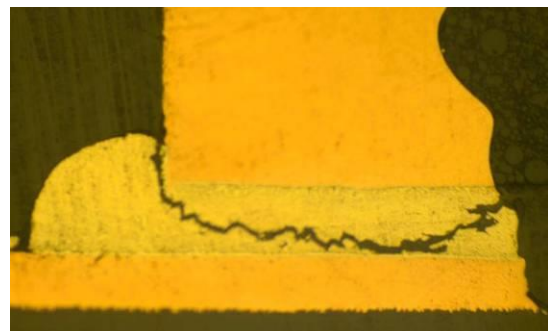
# Ductile Fatigue Cracks in Solder Joints



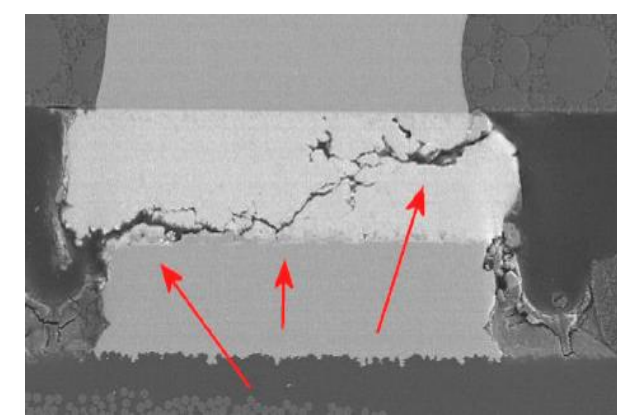
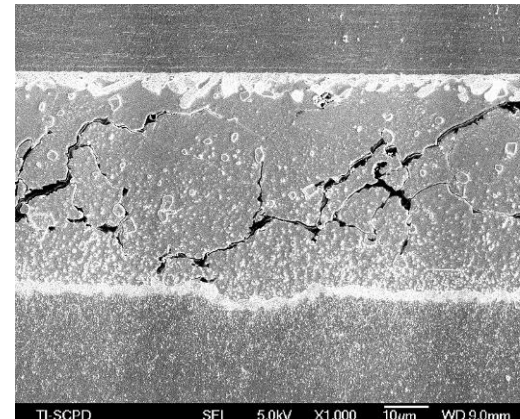
CBGA 29mm, 1.27mm pitch, 483 pads  
*Accelerated thermal cycling (0-100°C)*



Courtesy HDPUUG



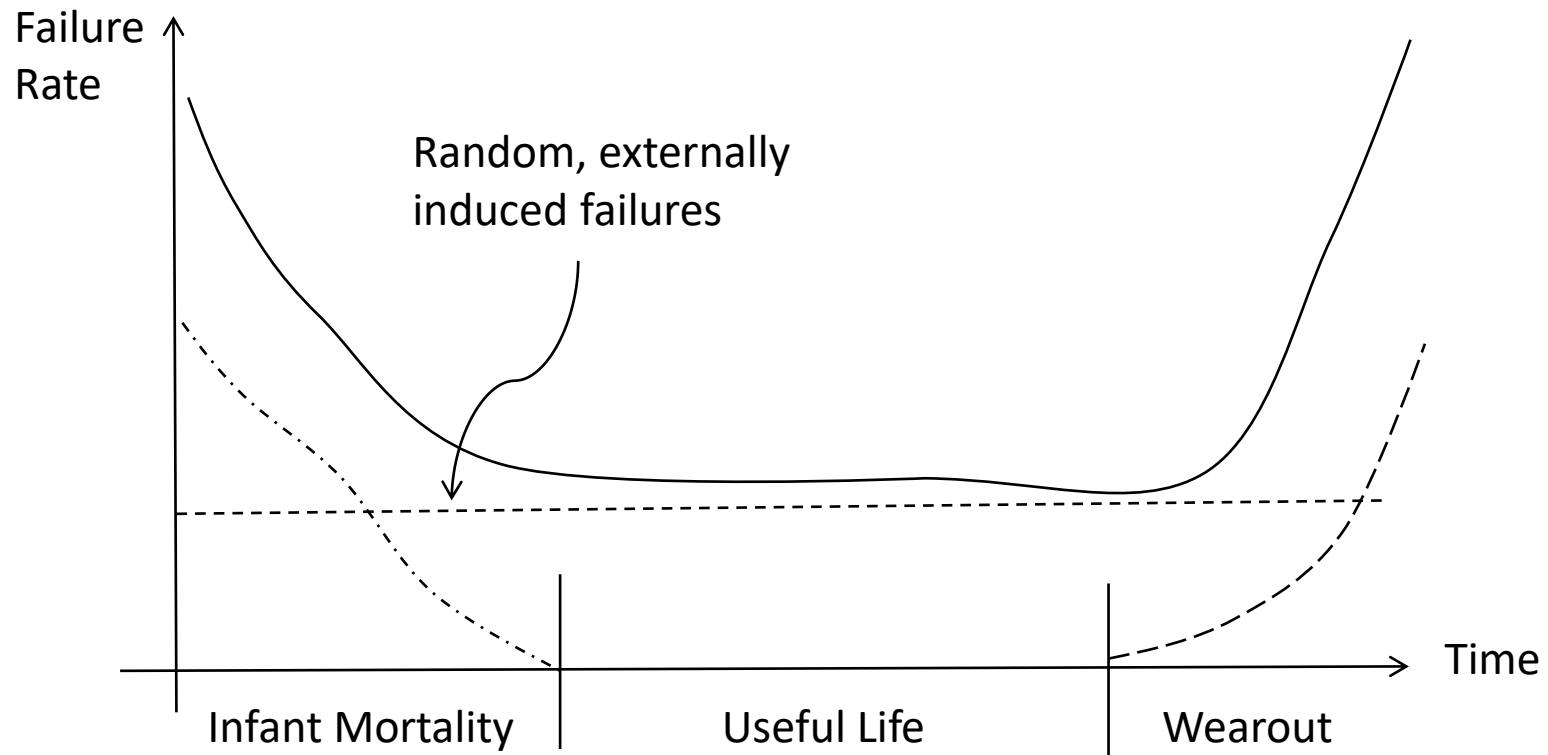
QFN, 0.5mm pitch, 64 I/Os, 4mm square  
*Accelerated thermal cycling (-40 to 125°C)*



Courtesy TI

# Environmental Testing and Statistical Failure Characterization

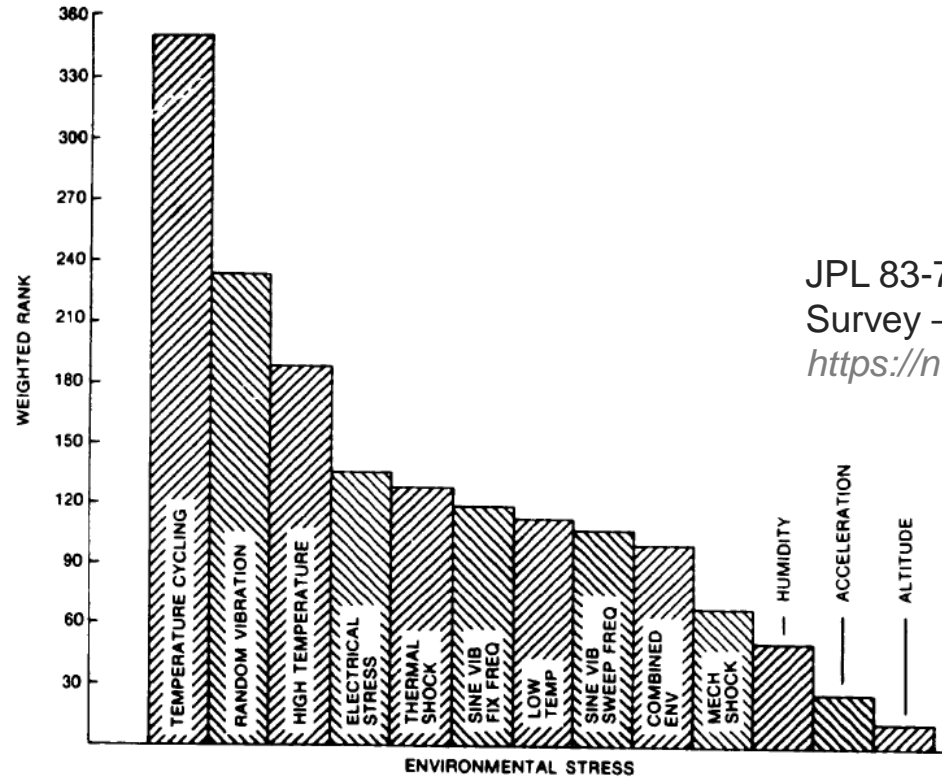
# Rates of Failure – “Bathhtub Curve”



# Introduction to Accelerated Degradation

- Rate of material degradation can be accelerated by increased
  - *Stress*: Mechanical/electrical/electrochemical
  - *Temperature*
- Accelerated testing causes *shorter time to failure without changing the physics of failure*
  - Enabled by understanding stress and temperature dependence of failure mechanisms

# Common Mechanical Tests for Electronic Packages

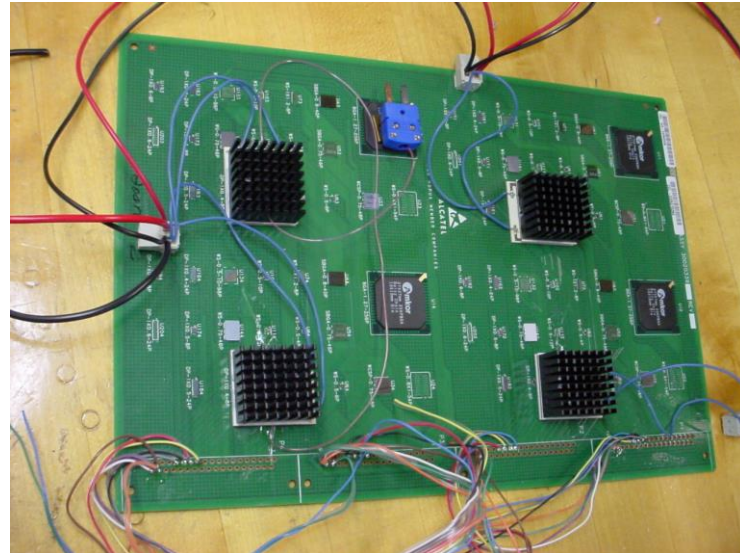


JPL 83-76 NASA Flight Electronic Environmental Stress Screening Survey –Source:  
<https://ntrs.nasa.gov/archive/nasa/casi.ntrs.nasa.gov/19840013934.pdf>

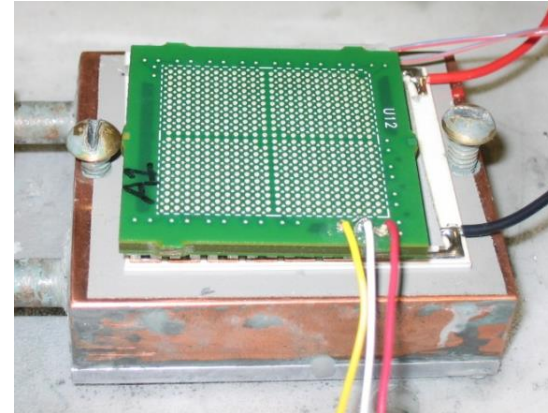
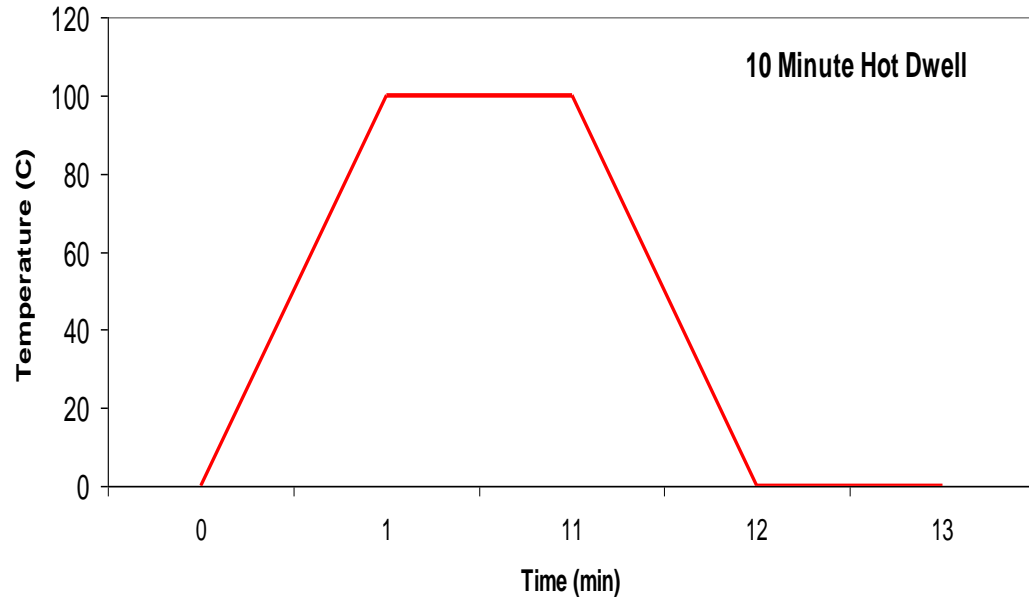
Figure 1. Effectiveness of Environmental Screens. (Ref. 1)

# Accelerated Tests

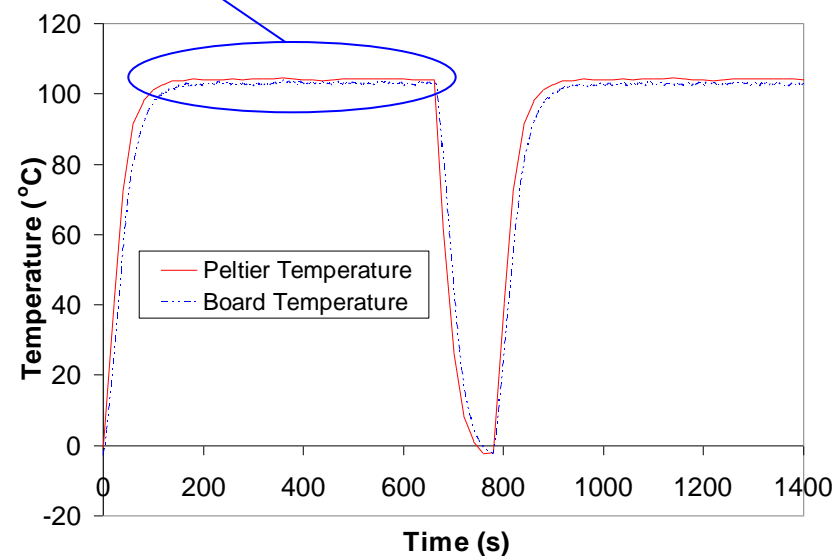
- Inducing Failure
  - Accelerated Thermal Cycling
  - Simulated Power Cycling
  - Power Cycling
  - Drop Test
  - Vibration Test
- Failure Analysis
  - Cross-section
  - Dye and Pry
  - X-ray, CSAM



# Accelerated Thermal and Power Cycling



Hot Dwell



Three temperature profiles

- 0°C to 100°C
- Hold time at 100°C
- 10, 30, and 60 minute hot dwells

# Weibull Distribution

$$R(t) = \exp[-(\lambda t)^\beta]$$

- Reliability

$$= \exp\left[-\left(\frac{t}{\eta}\right)^\beta\right]$$

- $\eta$ : characteristic life – time at which 63.2% of population will have failed
- $\beta$ : shape parameter (when  $\beta = 1$ , reduces to exponential distribution)

- CDF

$$F(t) = 1 - \exp\left[-\left(\frac{t}{\eta}\right)^\beta\right]$$

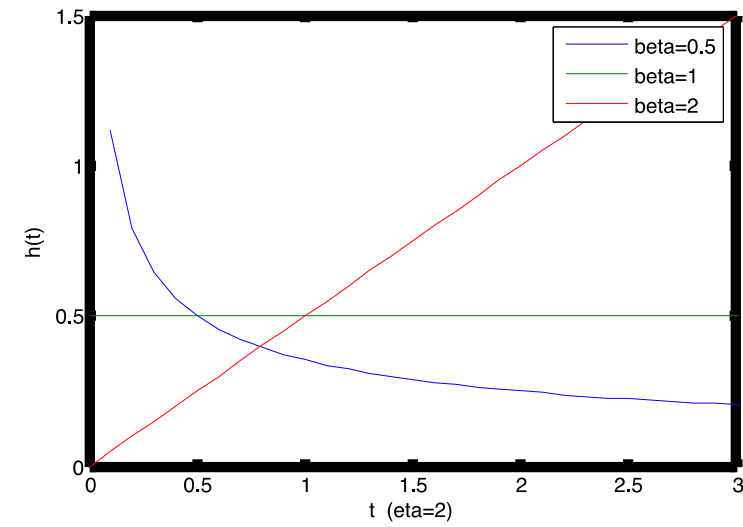
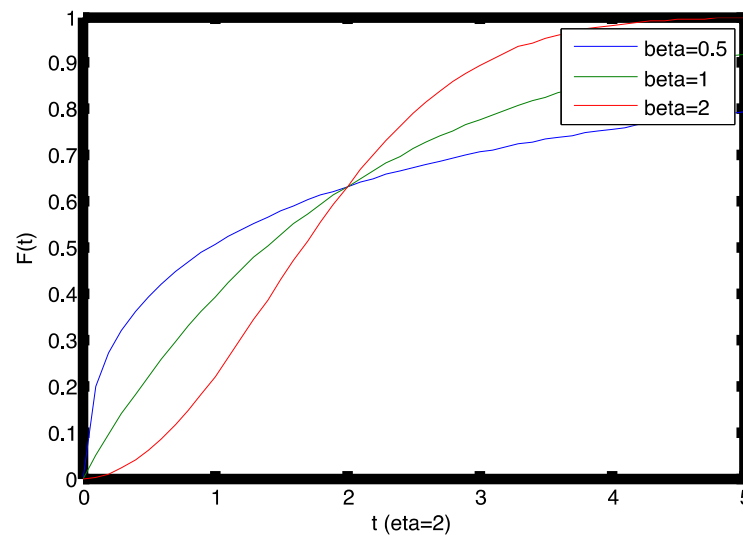
- PDF

$$f(t) = \begin{cases} \frac{\beta}{\eta^\beta} t^{\beta-1} \exp\left[-\left(\frac{t}{\eta}\right)^\beta\right] & (\text{for } t \geq 0) \\ 0 & (\text{for } t < 0) \end{cases}$$

- Hazard rate

$$h(t) = \frac{\beta}{\eta^\beta} t^{\beta-1}$$

# CDF and Hazard Rate Plots



# Weibull Linearization

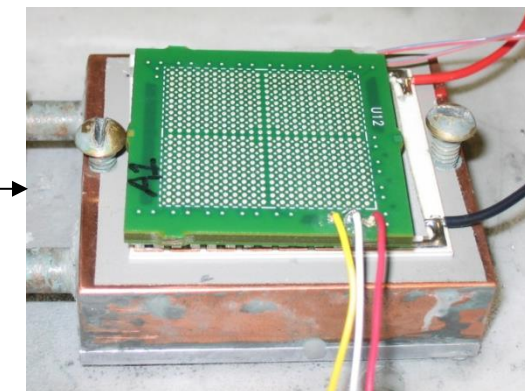
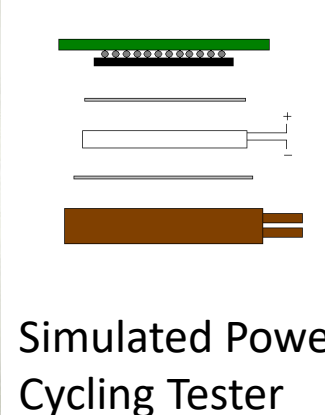
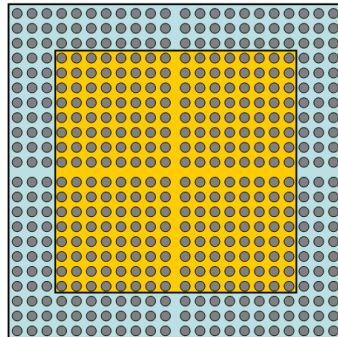
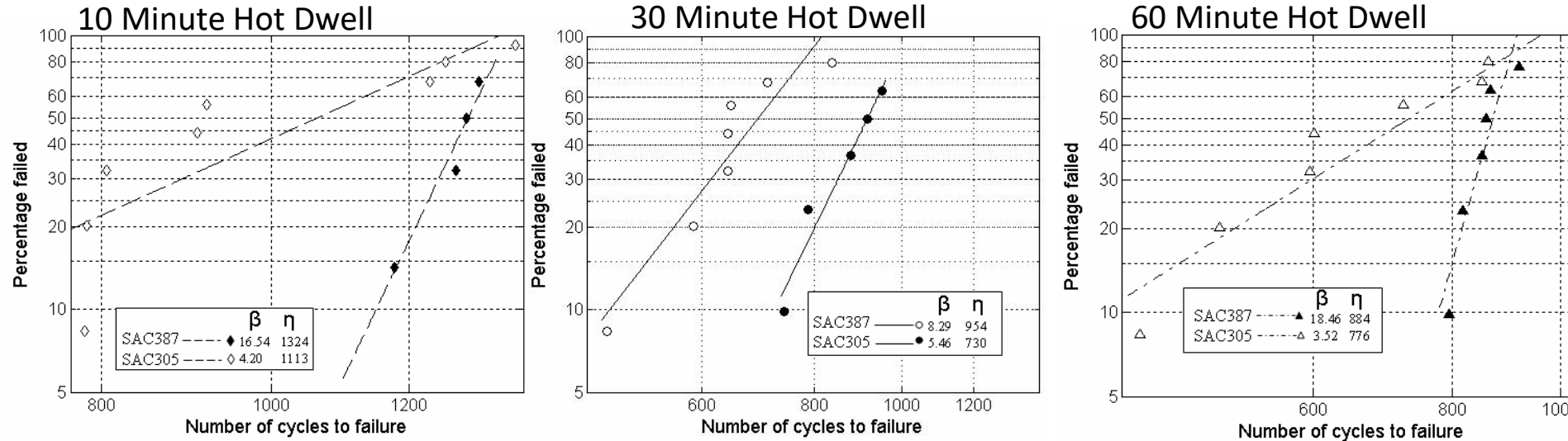
$$R(t) = 1 - F(t) = \exp \left[ - \left( \frac{t}{\eta} \right)^\beta \right]$$

$$\Rightarrow \ln[-\ln R(t)] = \beta \ln t - \beta \ln \eta$$

- Linearization makes fits and plots easy
- Slope=  $\beta$

# Statistical Characterization of Failures

Sn3.0Ag0.5Cu and Sn3.8Ag0.7Cu for 10, 30, 60 min Hot Dwell Times



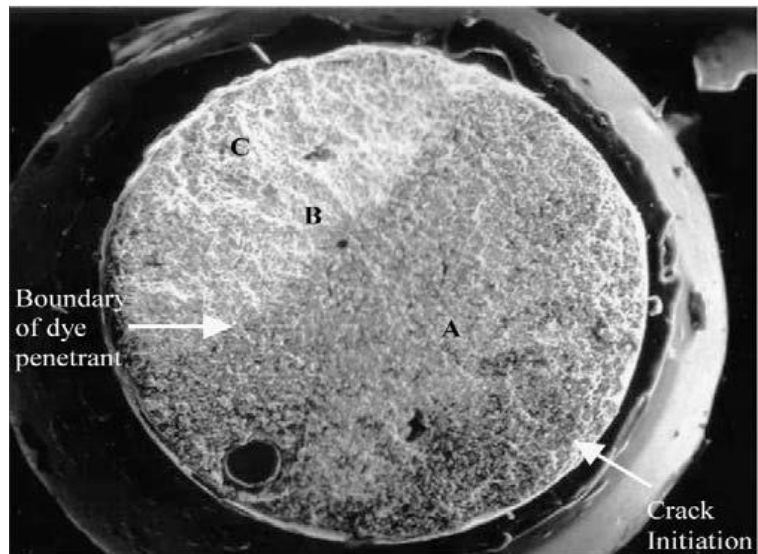
Chan et al., IEEE ECTC, 2007.

# Failure Analysis

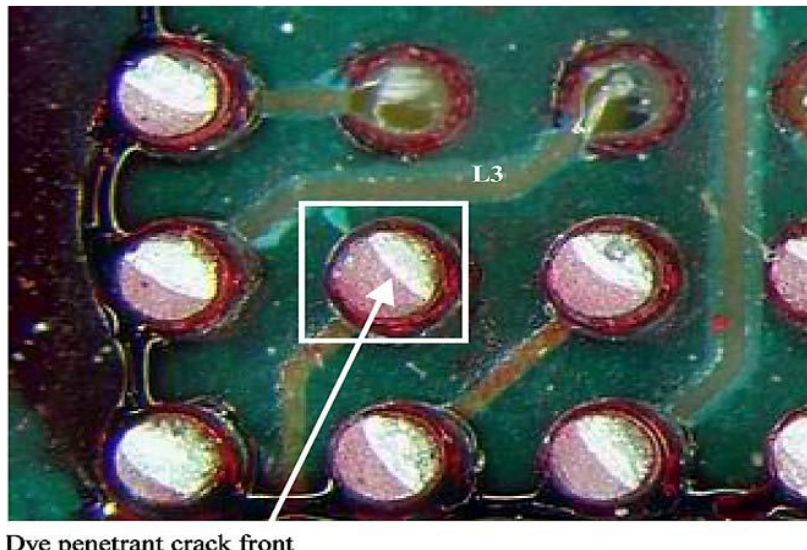
## Cross Section



## Fracture Morphology



## Dye and Pry

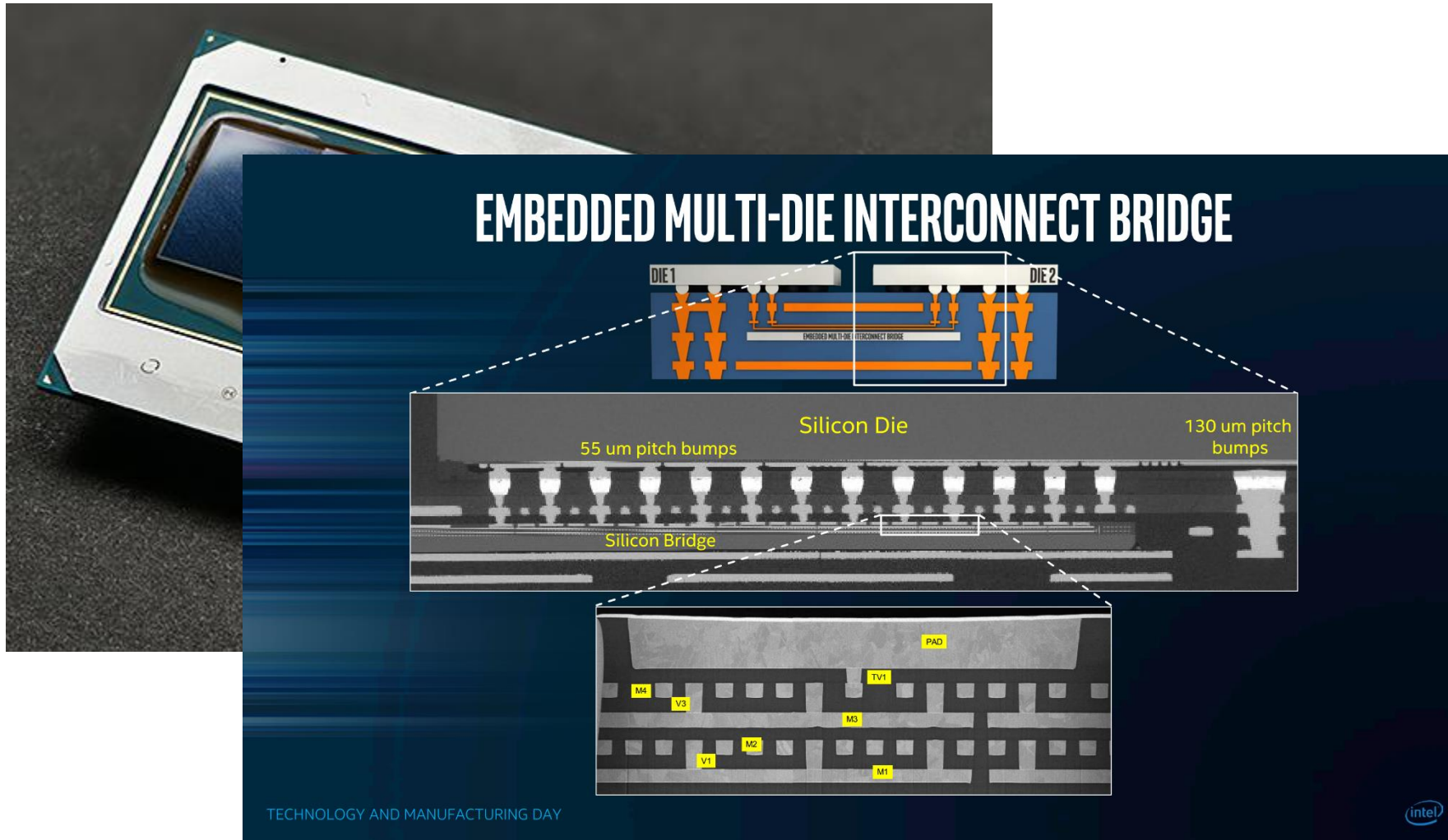


- A: Fatigue/Creep failure region with dye
- B: Fatigue/Creep failure region without dye
- C: Shear overload failure region

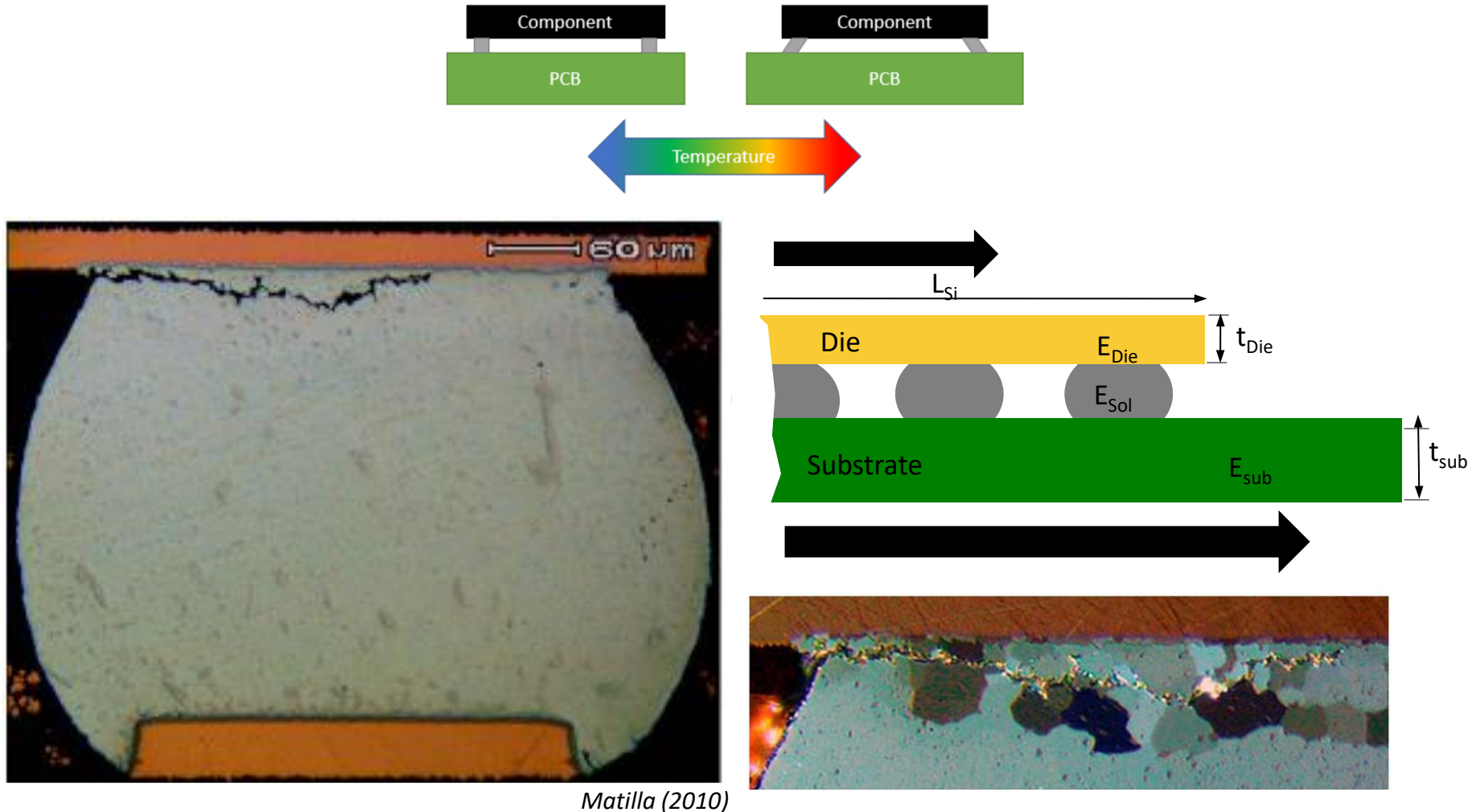
P. Towashiraporn, G. Subbarayan, C.S. Desai, "A Hybrid Model for Computationally Efficient Fatigue Fracture Simulations at Microelectronic Assembly Interfaces." *International Journal of Solids and Structures*, v 42, p 4468-4483, 2005.

# Ductile Fracture Case Study: Solder Joint Fatigue Life Characterization

# Motivation: Electronic Assemblies



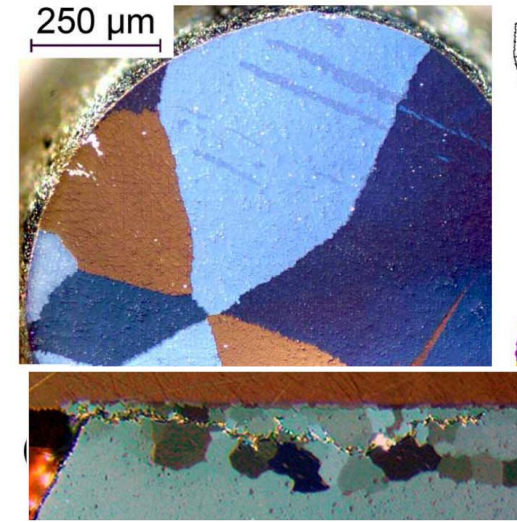
# Solder Joint Fatigue Fracture



# Motivation: Microstructure of Sn3.0Ag0.8Cu Solder Joints



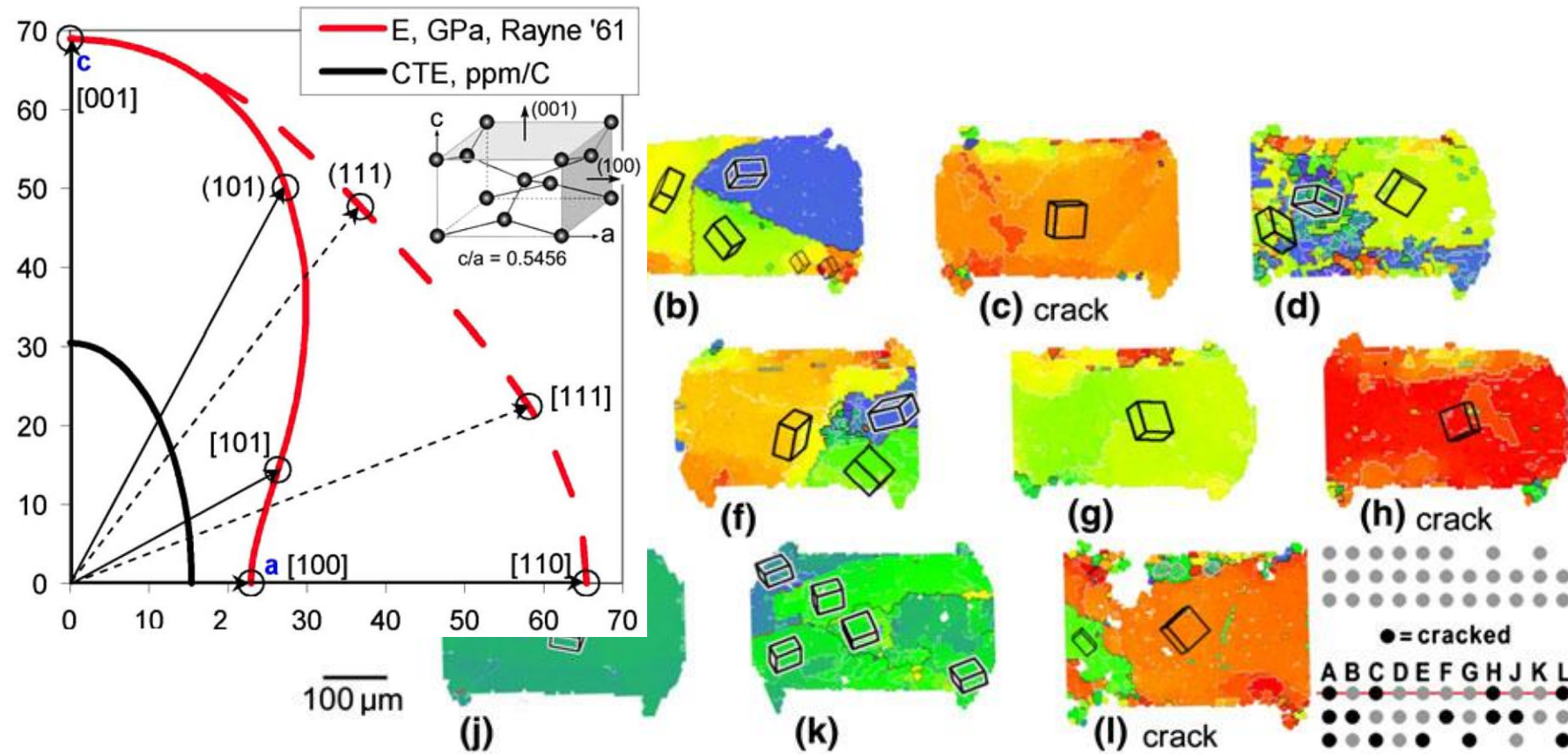
Bieler et al. (2008)



Matilla (2010)

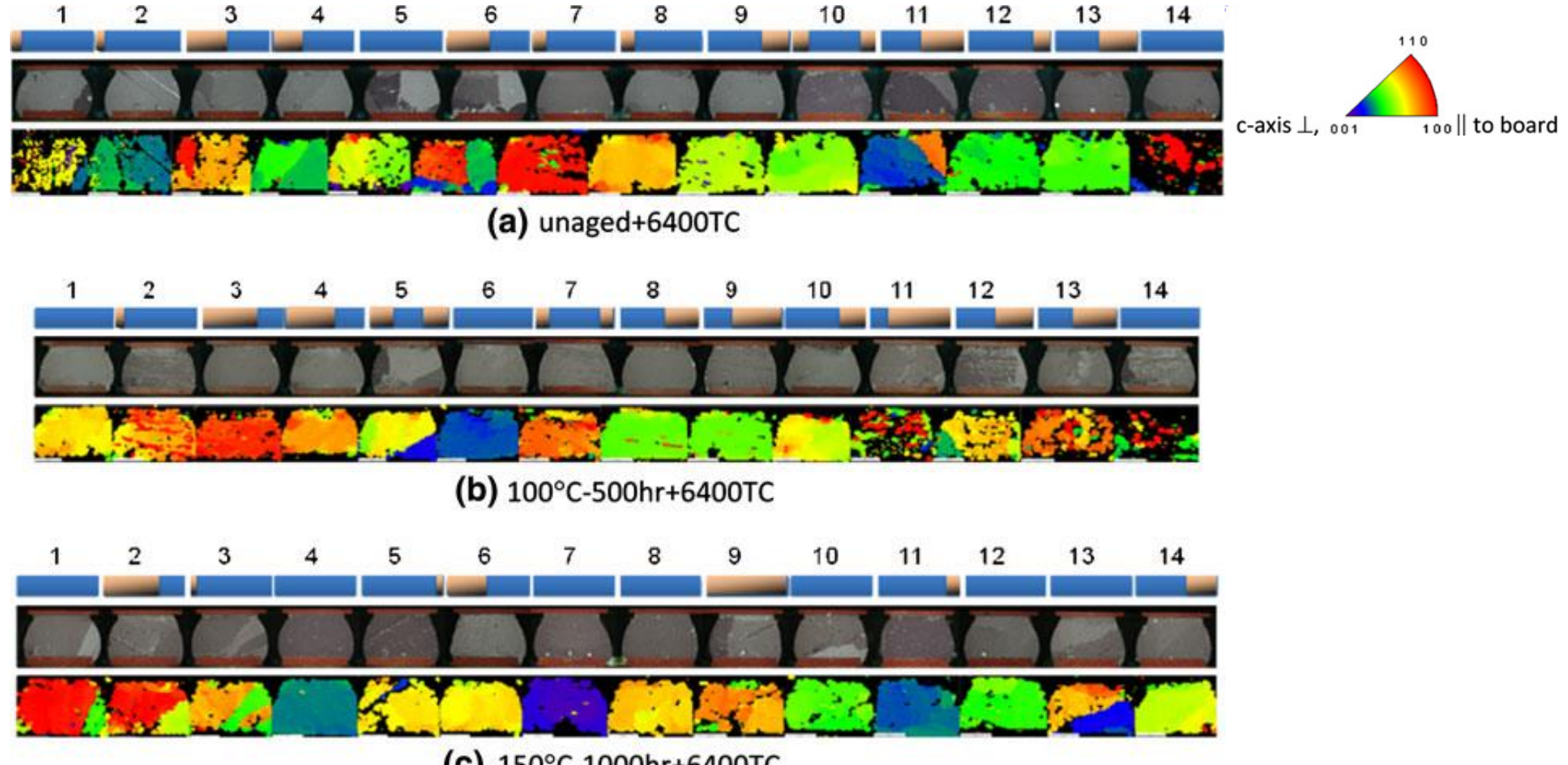
- SnAgCu solder joints have few grains and grain orientation known to influence fracture propensity
- Microstructure evolves ahead of the crack due to recrystallization and cracks largely follow macro stress and geometry

# Motivation: Effect of Sn Anisotropy



T.R. Bieler et al., "Influence of Sn Grain Size and Orientation on the Thermomechanical Response and Reliability of Pb-free Solder Joints," *IEEE Transactions on Components and Packaging Technologies* 31, no. 2 (6, 2008): 370-381.

# Motivation: Microstructural Effects on Fatigue Life

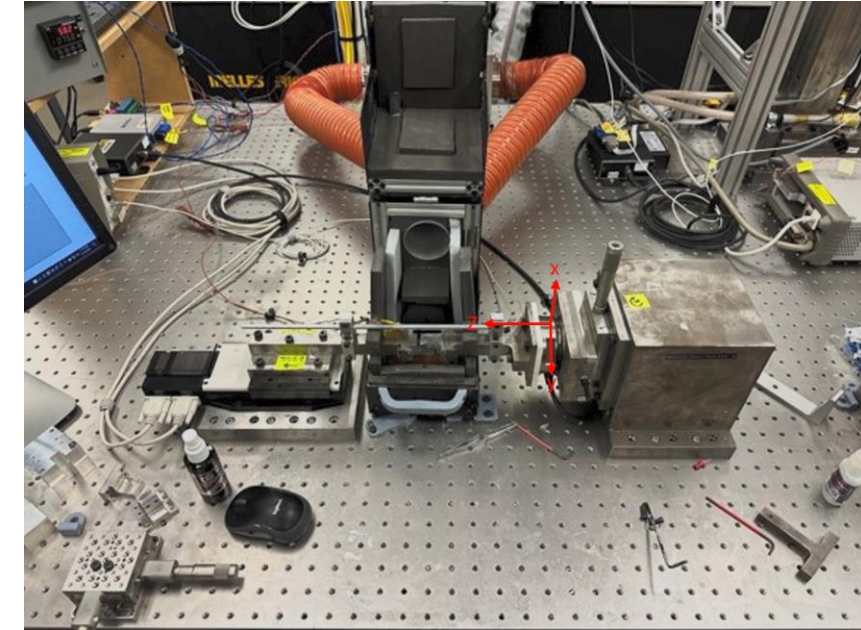


B. Zhou, T. R. Bieler, T. Lee, and K. C. Liu, "Crack Development in a Low-Stress PBGA Package due to

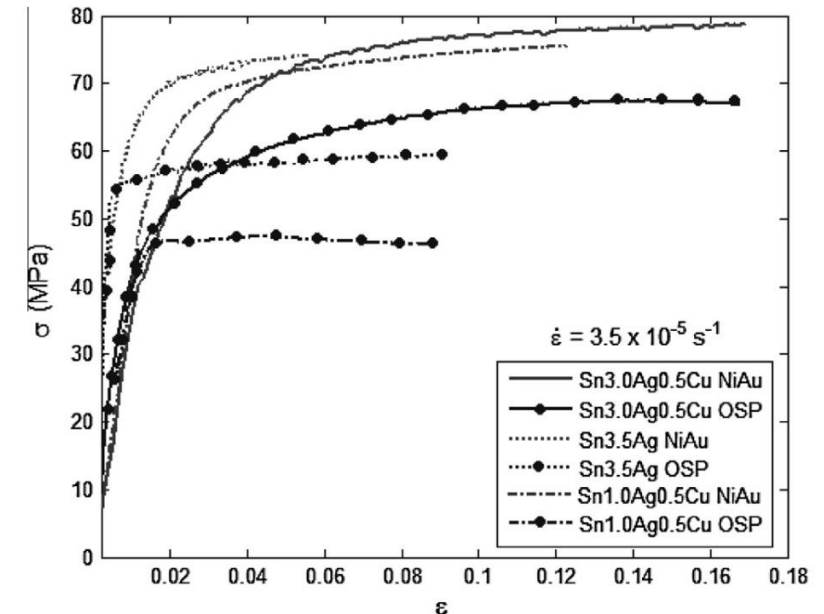
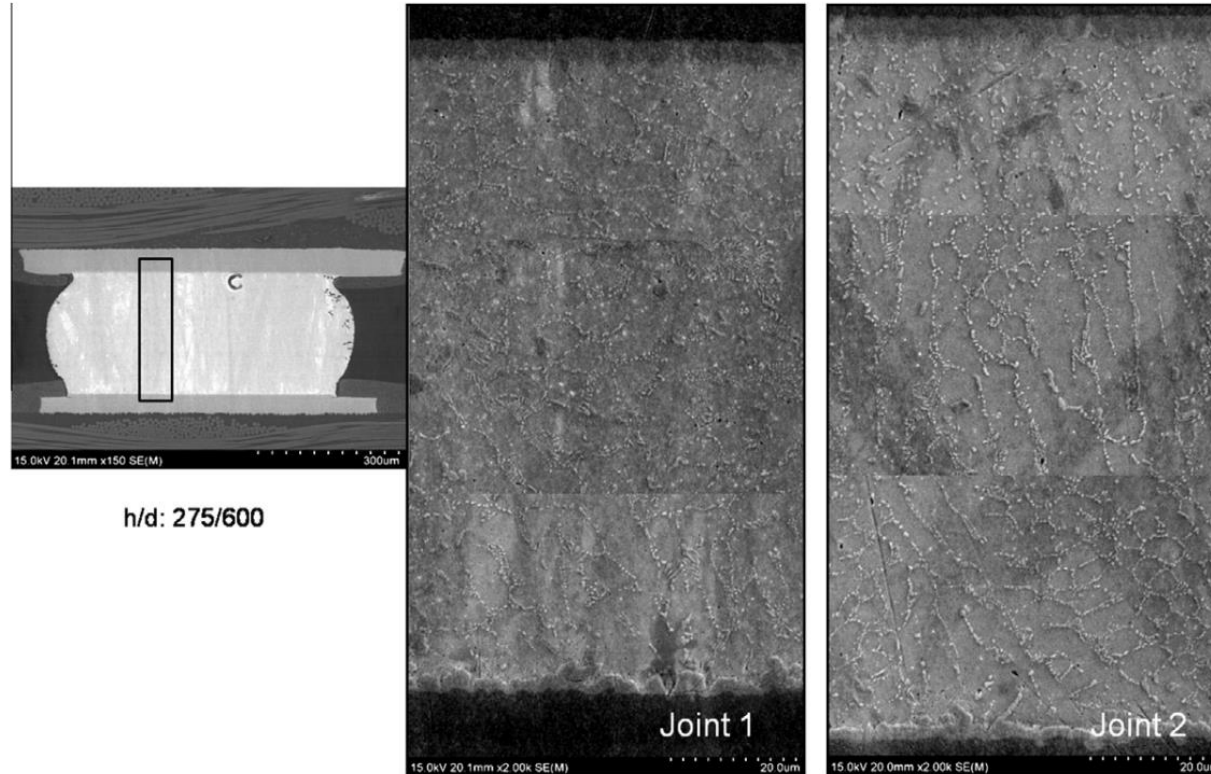
2024-10-19 ISM PDC on Reliability Continuous Recrystallization Leading to Formation of Preferred Orientations with [001] Parallel to the Interface,"  
*Journal of electronic materials*, pp. 1-11, 2010.

# Experimental Setup for Mechanical Characterization of Solder Alloys

- Why build a custom tester instead of a commercial solution?
  - Joint scale testing
    - Captures effect of microstructure due to pad finish or joint size
  - Closed-loop position control
    - Necessary for joint-scale testing
  - Allows reversed loading for fatigue testing
    - No universal joints to cause backlash
  - Six-axis load cell to correct misalignment
    - Z axis: range of  $\pm 200$  N & resolution of 0.025 N
    - X & Y axes: range of  $\pm 65$  N & resolution of 0.0125 N
    - Manual stages to eliminate off-axis loads and moments
  - Thermal chamber capable of RT-250 C testing
  - LabView software for ease of customization
- Tester controls displacement at sample to sub-micron precision
  - Capacitance sensor: range of 250  $\mu\text{m}$  and a resolution of 7.5 nm
- **Tester controls displacement at sample to sub-micron precision**

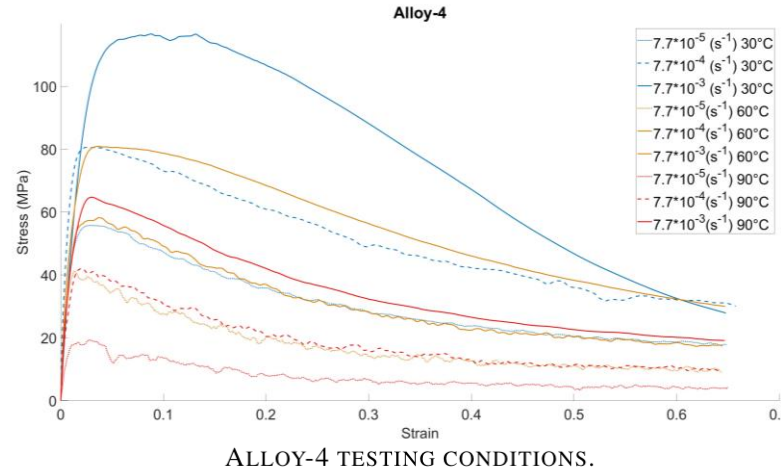


# Need for Joint Scale Testing: Effect of Pad Finish

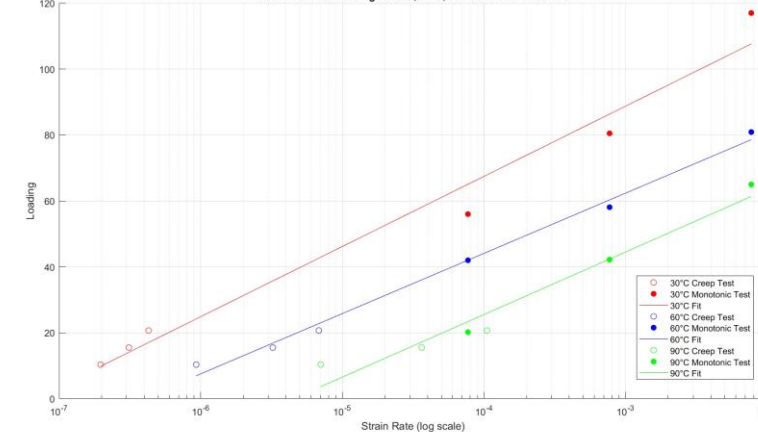
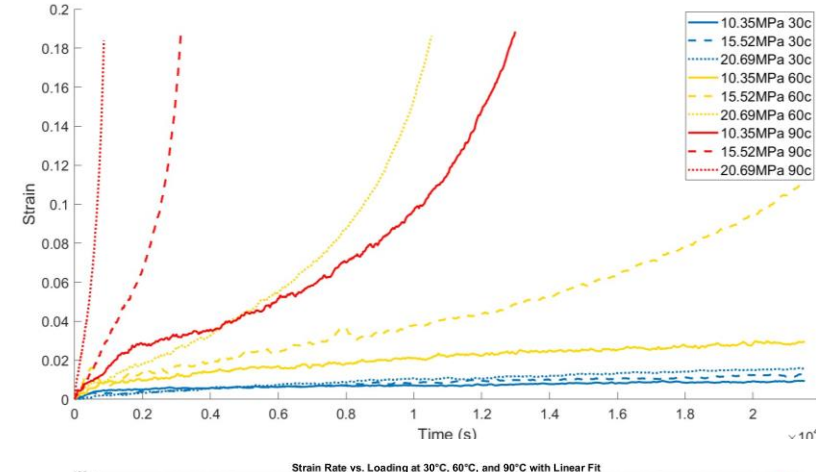


S. Chavali, G. Subbarayan, A. Bansal, and M. Ahmad, "Effect of Pad Surface Finish and Reflow Cooling Rate on the Microstructure and the Mechanical Behavior of SnAgCu Solder Alloys," *Microelectronics Reliability*, vol. 53, no.6, pp. 892-898, 2013

# Monotonic Shear and Creep Shear Characterization

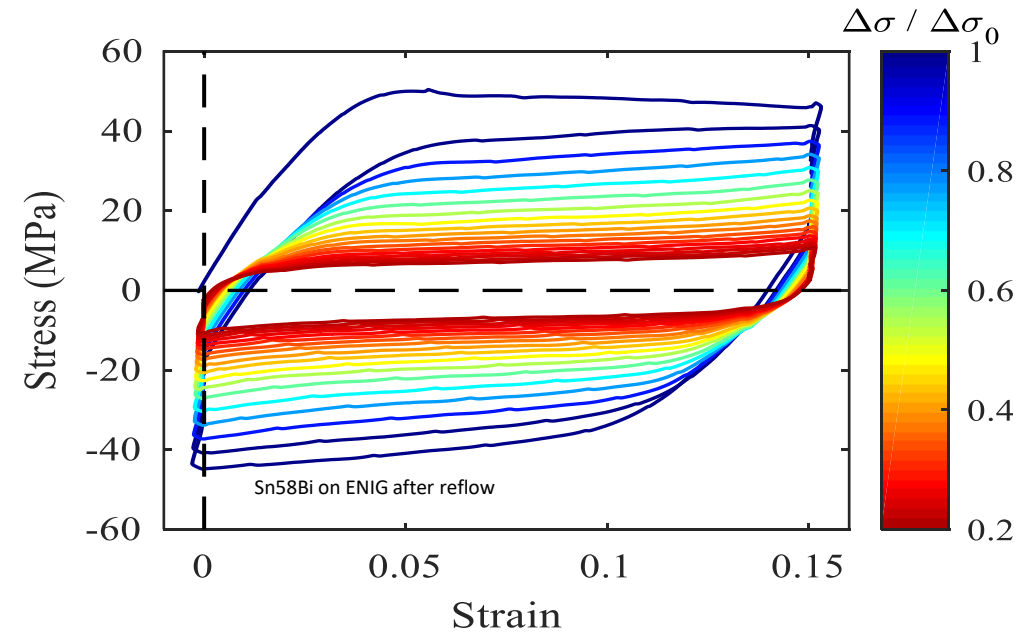


Alloy-4		
Temperature Condition	Monotonic Strain rate Condition	Creep Loading Condition
30°C	$7.7 \cdot 10^{-5} \text{ s}^{-1}$ (0.02μm/s)	10.35 Mpa (20N)
	$7.7 \cdot 10^{-4} \text{ s}^{-1}$ (0.2μm/s)	15.52 Mpa (30N)
	$7.7 \cdot 10^{-3} \text{ s}^{-1}$ (2μm/s)	20.69 Mpa(40N)
60°C	$7.7 \cdot 10^{-5} \text{ s}^{-1}$ (0.02μm/s)	10.35 Mpa (20N)
	$7.7 \cdot 10^{-4} \text{ s}^{-1}$ (0.2μm/s)	15.52 Mpa (30N)
	$7.7 \cdot 10^{-3} \text{ s}^{-1}$ (2μm/s)	20.69 Mpa(40N)
90°C	$7.7 \cdot 10^{-5} \text{ s}^{-1}$ (0.02μm/s)	10.35 Mpa (20N)
	$7.7 \cdot 10^{-4} \text{ s}^{-1}$ (0.2μm/s)	15.52 Mpa (30N)
	$7.7 \cdot 10^{-3} \text{ s}^{-1}$ (2μm/s)	20.69 Mpa(40N)

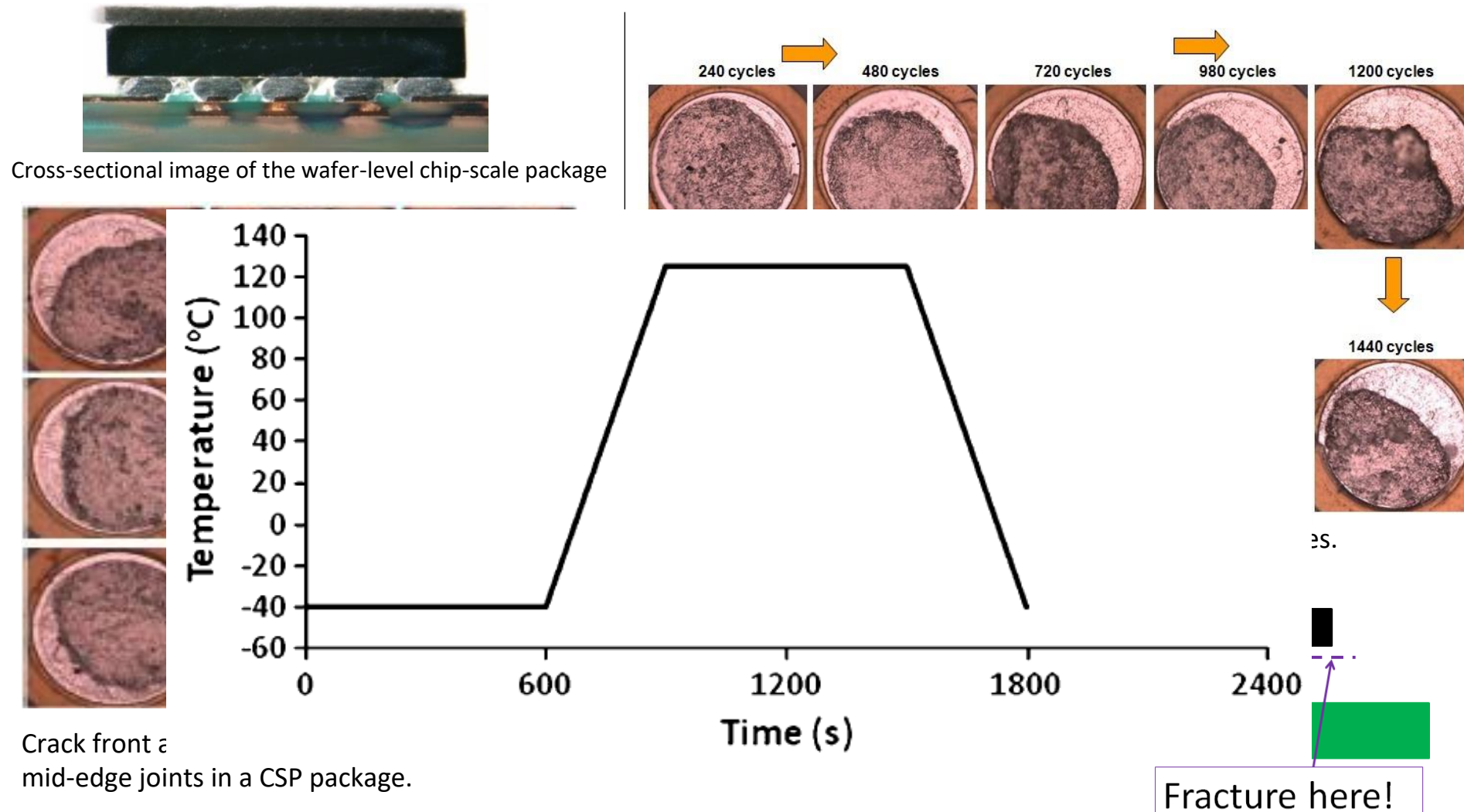


- Correlation of stress-strain rate response for Alloy-4 from monotonic and creep tests.

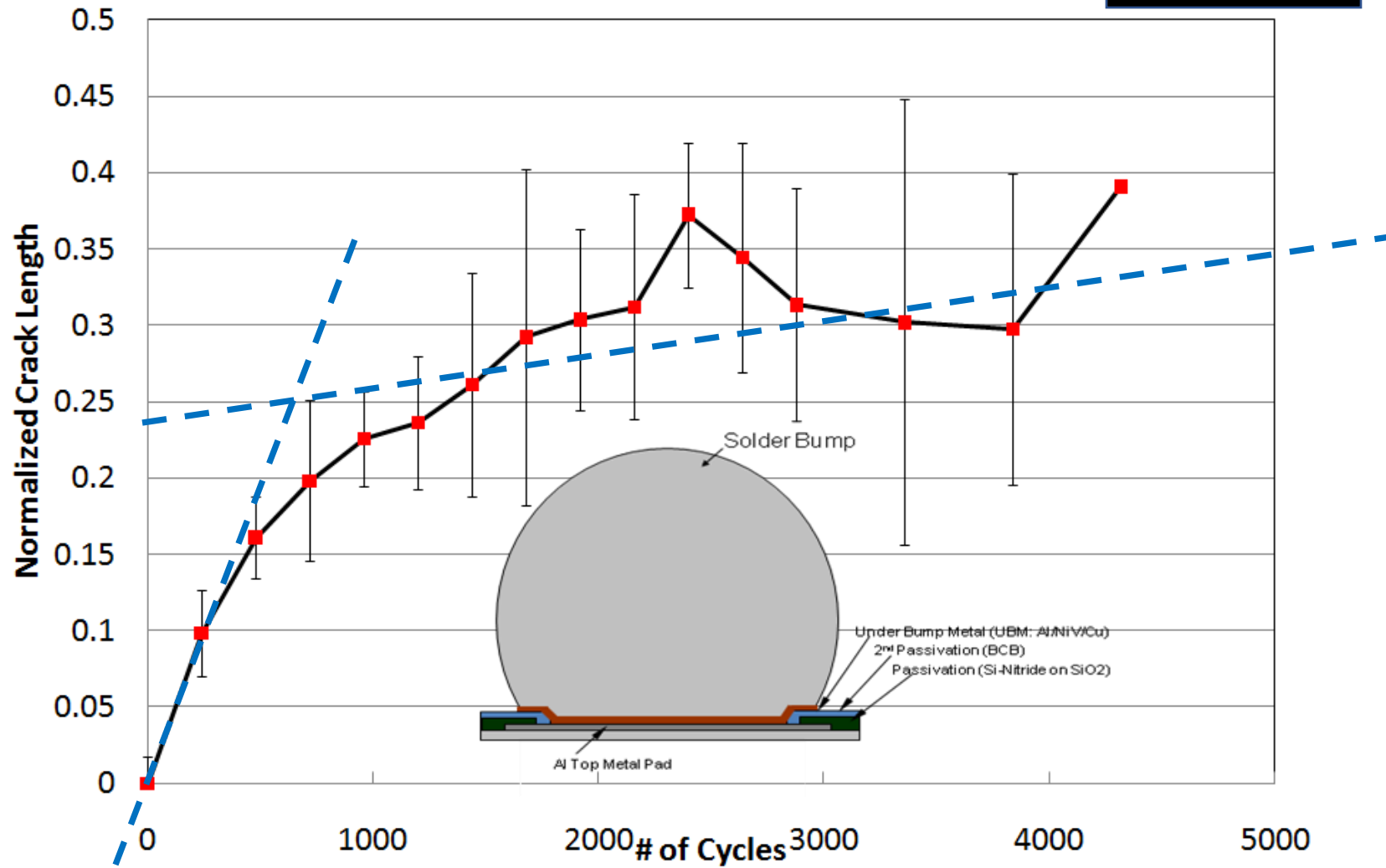
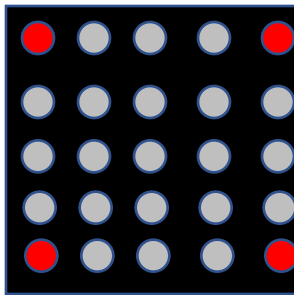
# Cyclic Fatigue Characterization



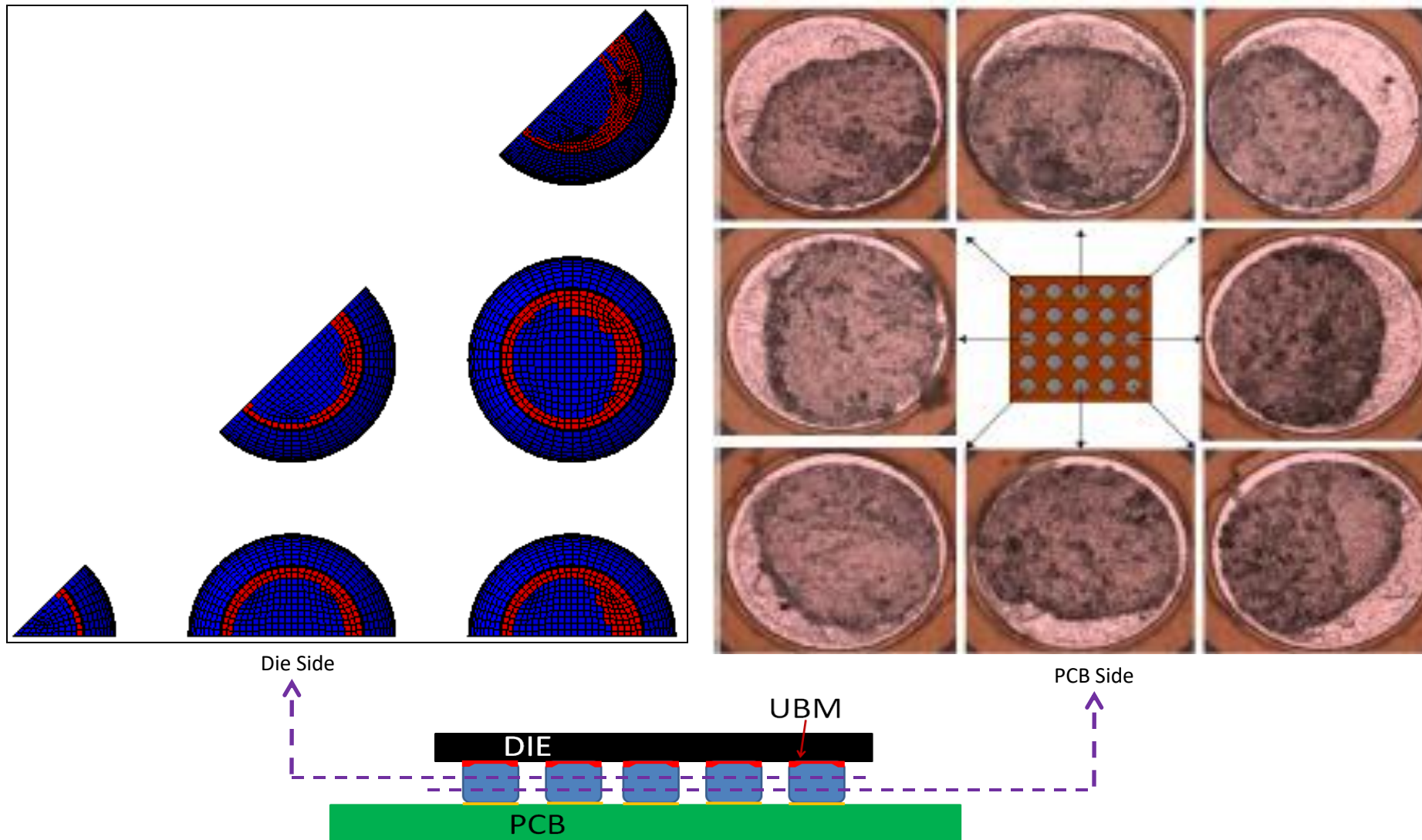
# Fatigue Fracture under Thermal Cycling



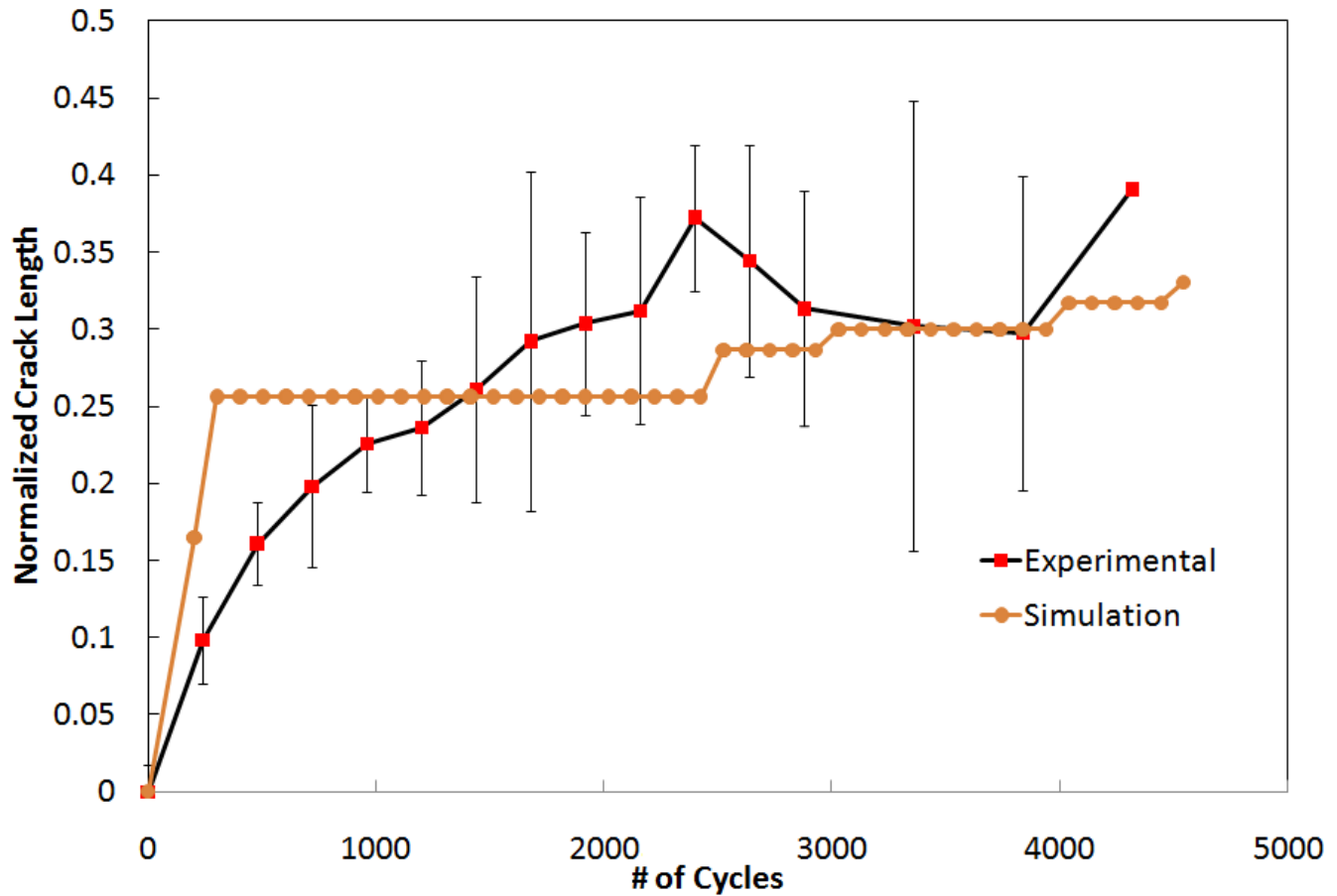
# Crack Growth of Corner Joint



# Simulated Fracture at 4747 Cycles



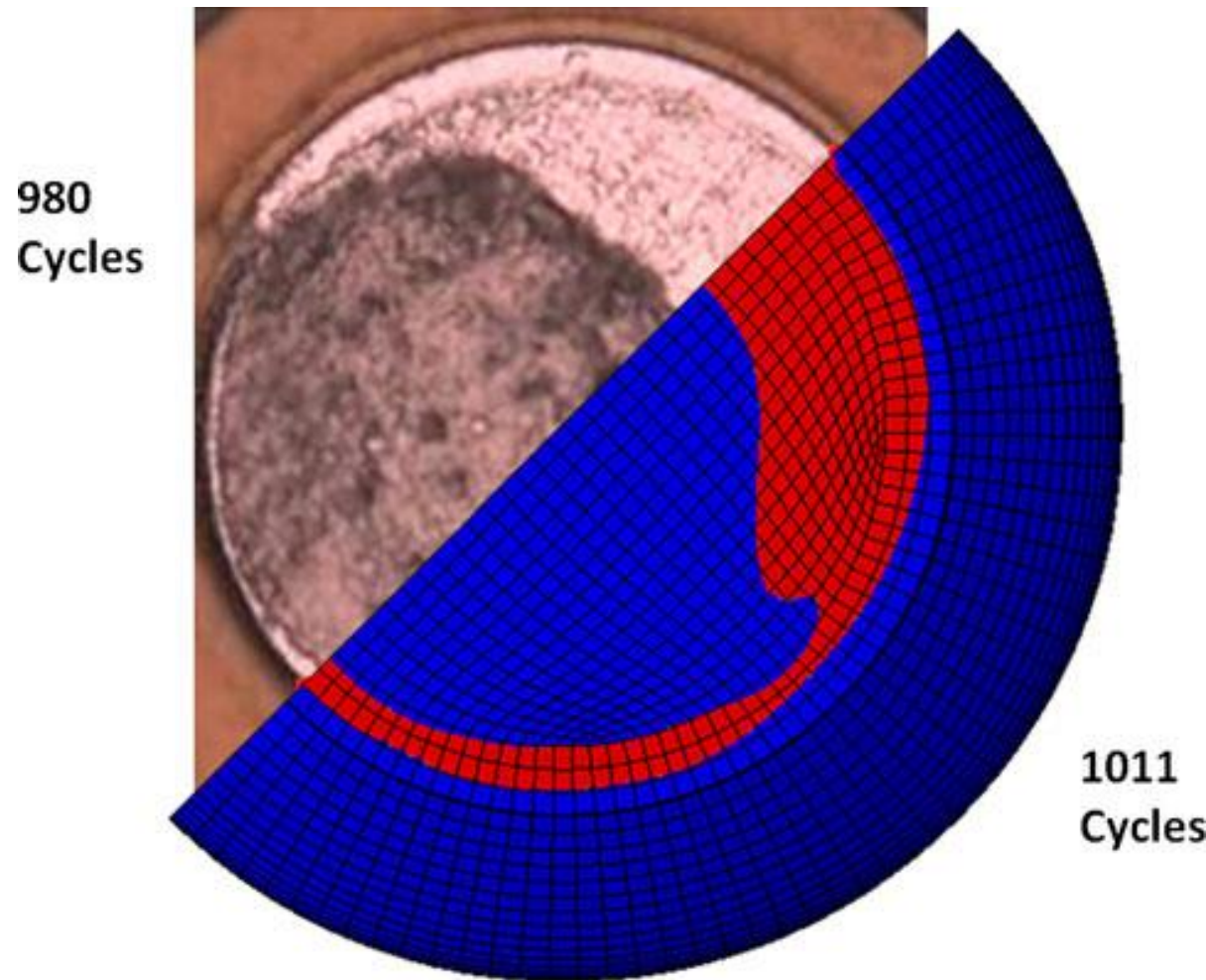
# Comparison between Experimental and Simulated Crack Lengths



Crack growth statistics of the simulated and experimental results.

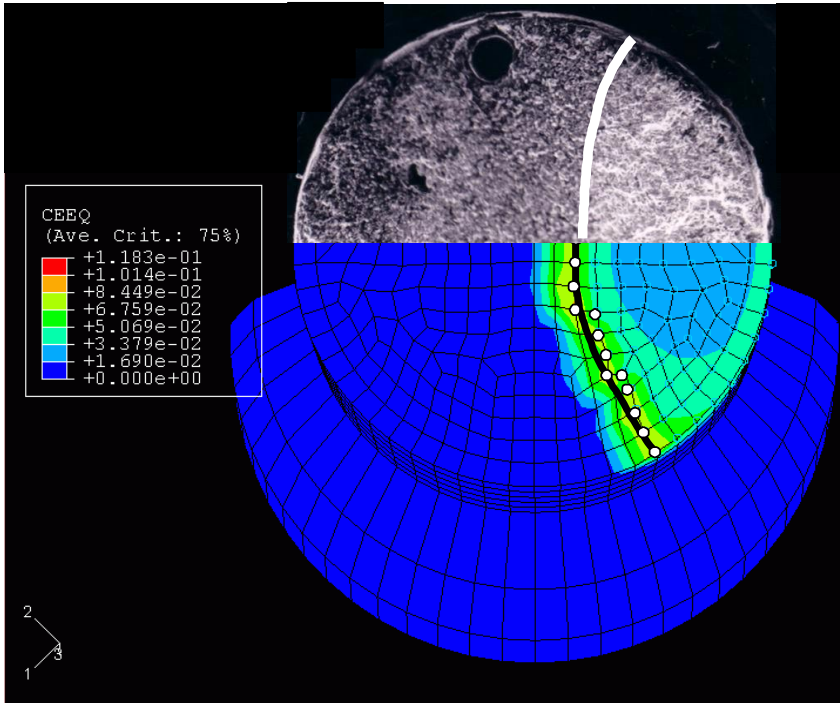
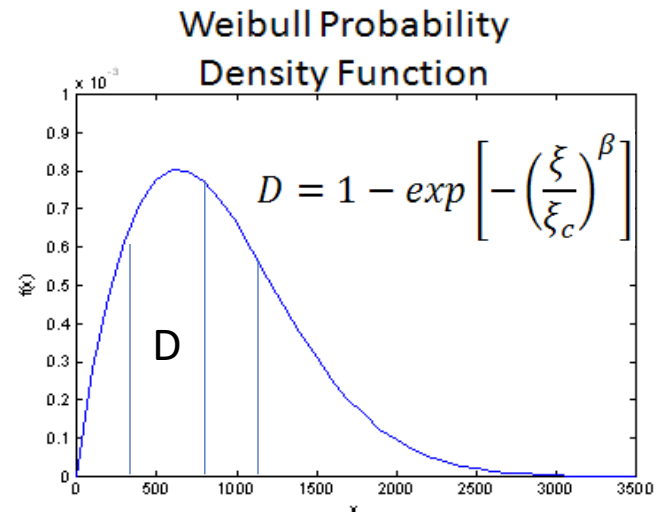
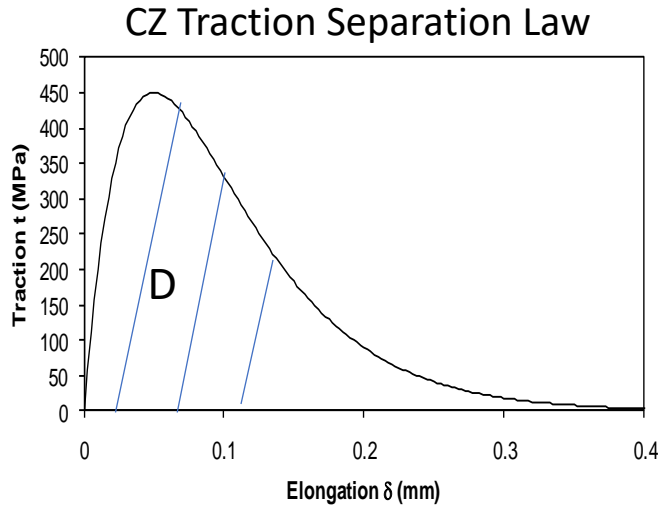
D. Chan, G. Subbarayan, and L. Nguyen, "Maximum-Entropy Principle for Modeling Damage and Fracture in Solder Joints," Journal of Electronic Materials, vol. 41, no. 2, pp. 398-411, Dec. 2011.

# Experiment vs. Finite Element Model



D. Chan, G. Subbarayan, and L. Nguyen, "Maximum-Entropy Principle for Modeling Damage and Fracture in Solder Joints," Journal of Electronic Materials, vol. 41, no. 2, pp. 398-411, Dec. 2011.

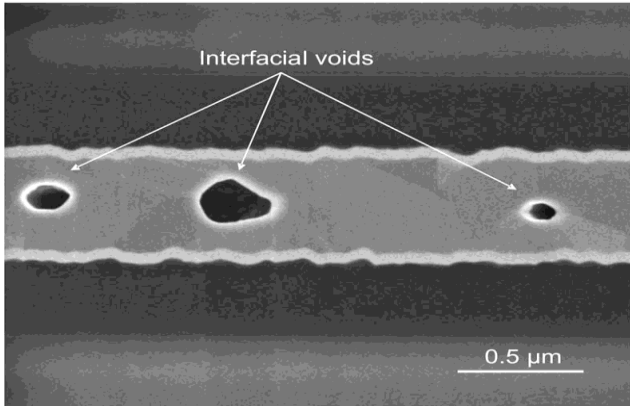
# Fracture in Sn40Pb Solder Joints



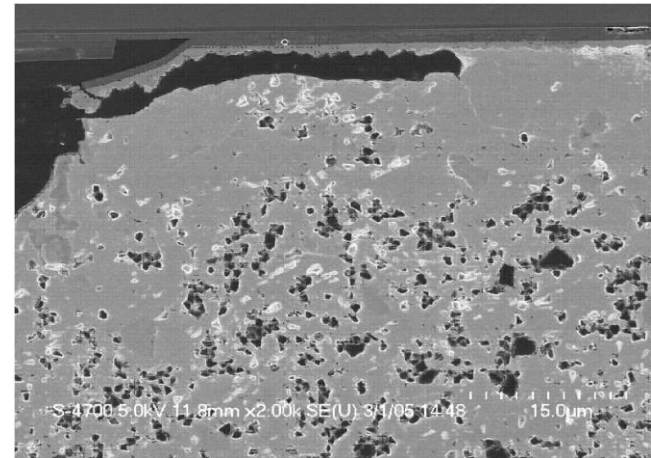
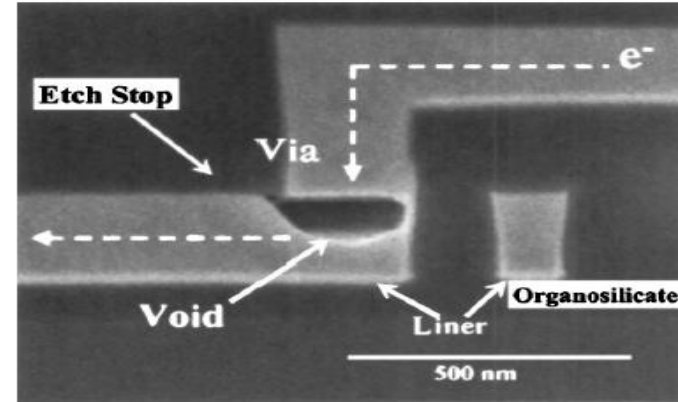
P. Towashiraporn, G. Subbarayan, and C. Desai, "A hybrid model for computationally efficient fatigue fracture simulations at microelectronic assembly interfaces," *International Journal of Solids and Structures*, vol. 42, no. 15, pp. 4468-4483, Jul. 2005.

# Diffusion Driven Failures: Electromigration and IMC Growth

# Diffusion and Electromigration Voiding

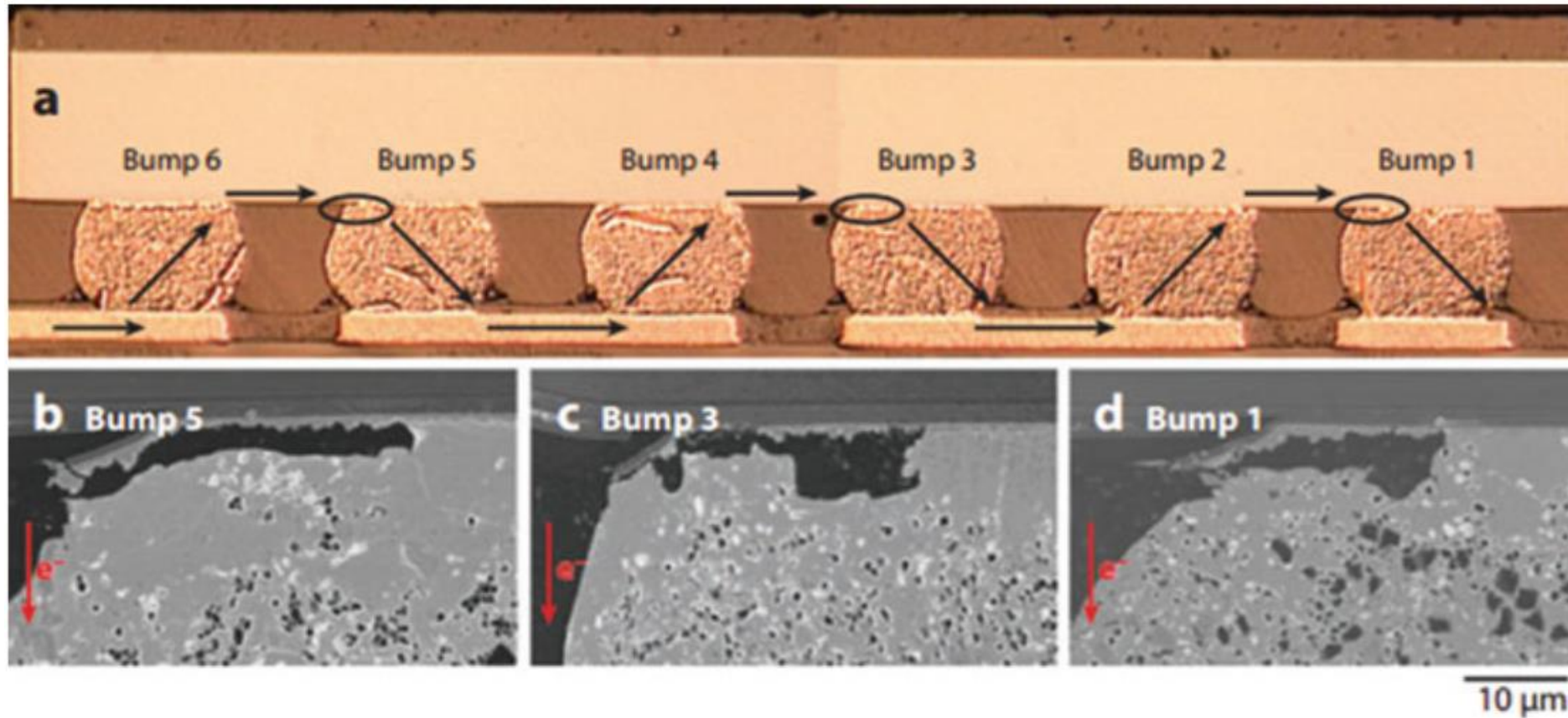


Leon, 2004



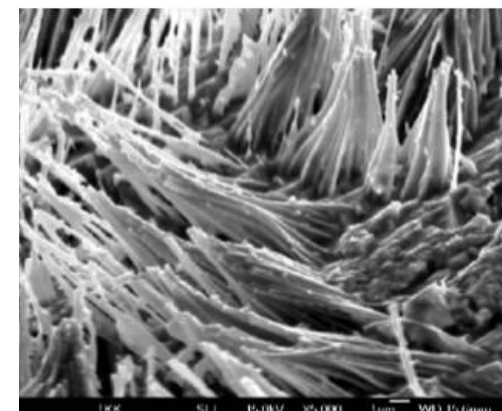
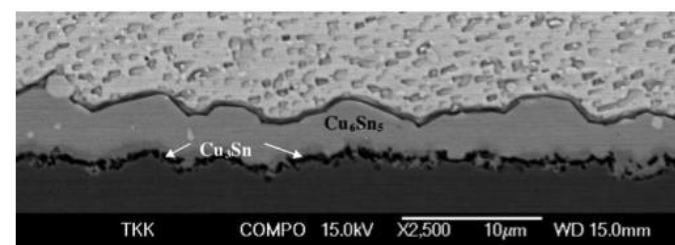
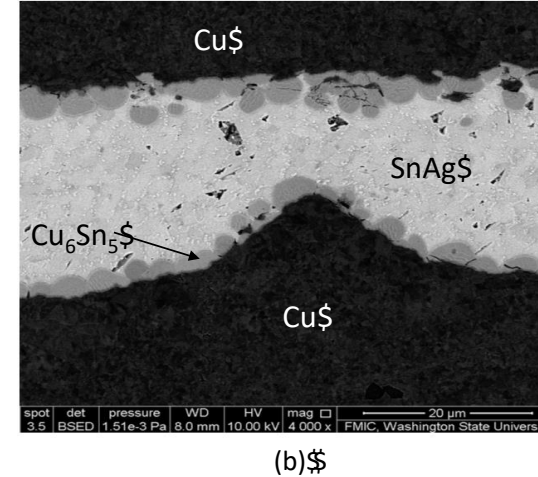
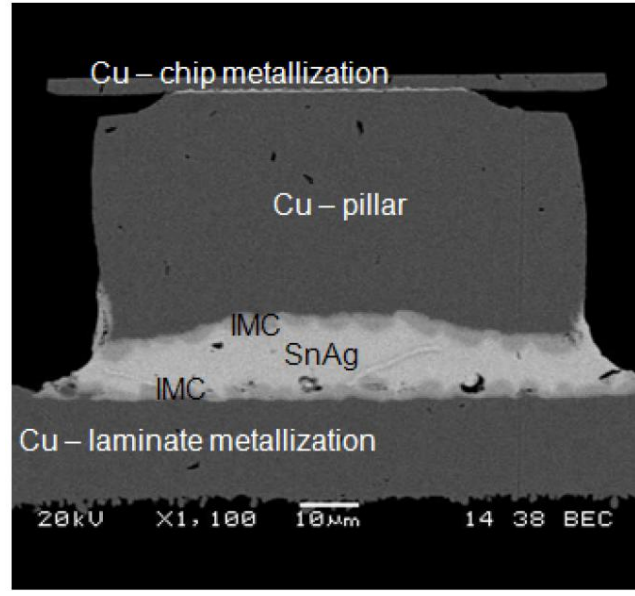
Tu et al., 2006

# Electromigration in Solder Joints



Yeh et al., 2002

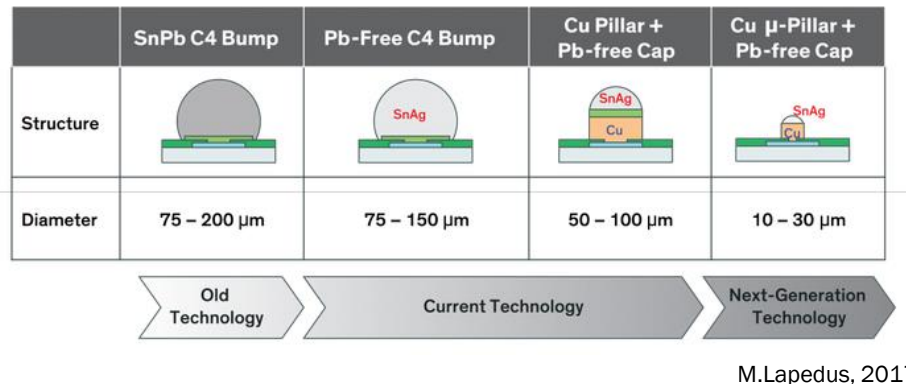
# Diffusion, Reaction and Interfacial Growth



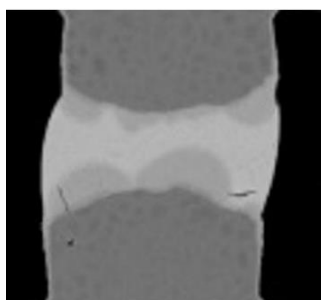
Laurila et al., 2005

# Motivation: Effect of Solder Joint Scaling on Electromigration Risk

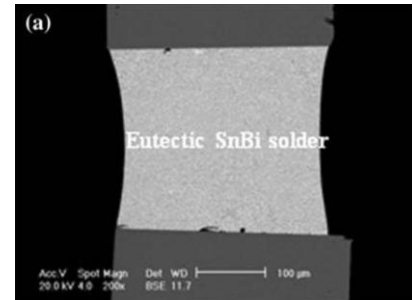
- Trend towards interconnects with finer pitch due to bandwidth and power efficiency requirements



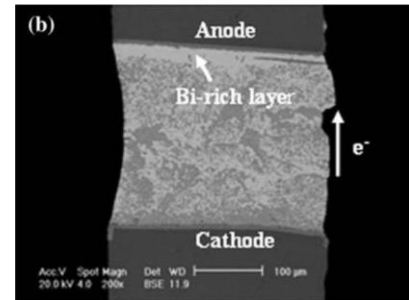
- Phase evolution phenomena can be a significant reliability concern as scale of interconnects reduce



150 °C  
1000 h



$5 \times 10^3 \text{ A/cm}^2$   
75 °C  
576 h



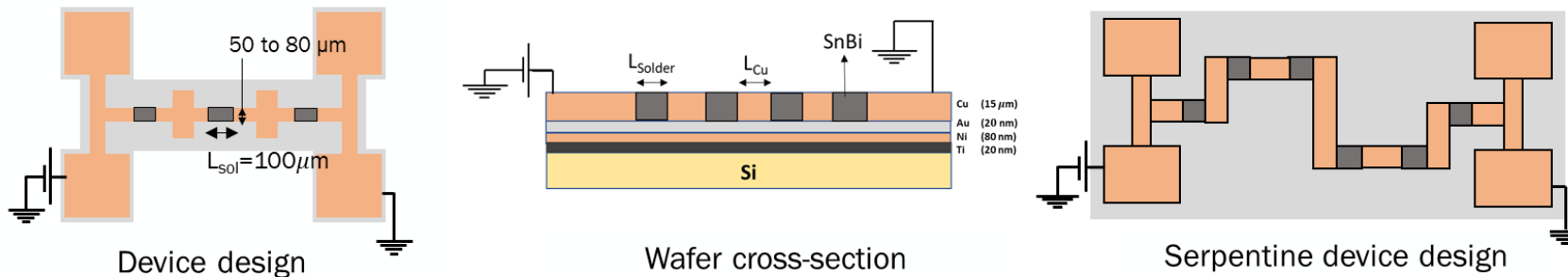
X. Gu and Y. Chan, 2008

# Electromigration Case Study: In-Line Test of SnBi Solder Joint

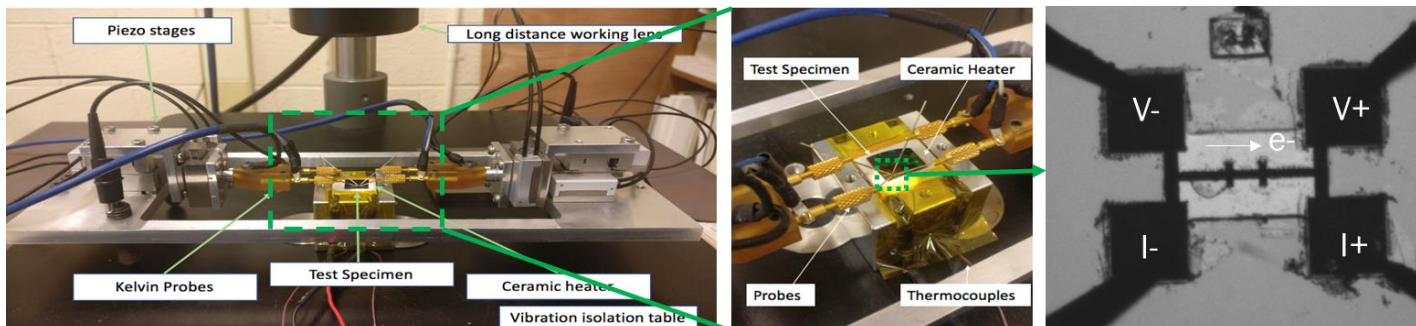
C. Jois, P.-E. Chou and G. Subbarayan, "In-Line Test Structures and Non-destructive Characterization of Electromigration-Driven Phase Evolution in Microscale Solder Joints", *Journal of Electronic Materials* (2024)

# In-Line Test Device Design and Fabrication

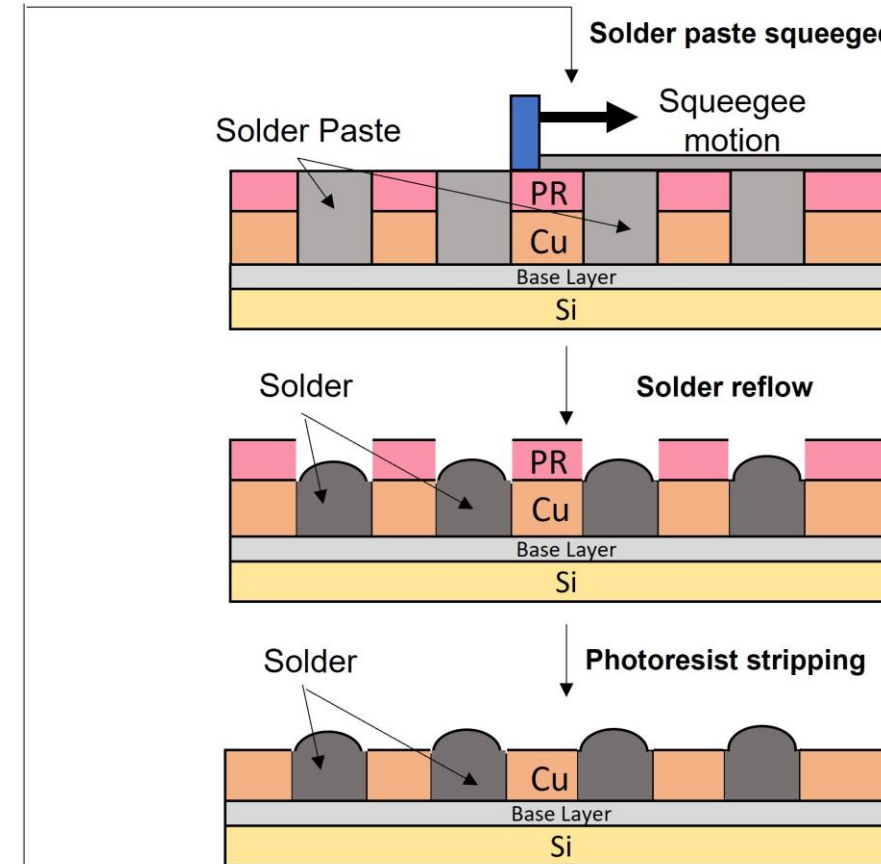
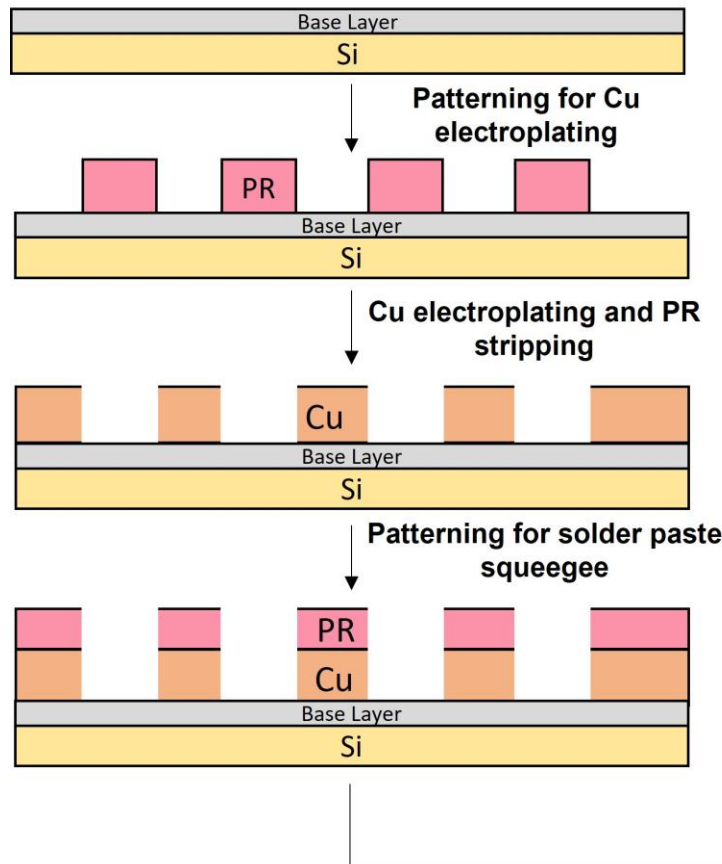
- In-Line test structures designed to observe effect of current crowding



- Custom-built experimental rig with ceramic heater capable of in-situ/ex-situ observations

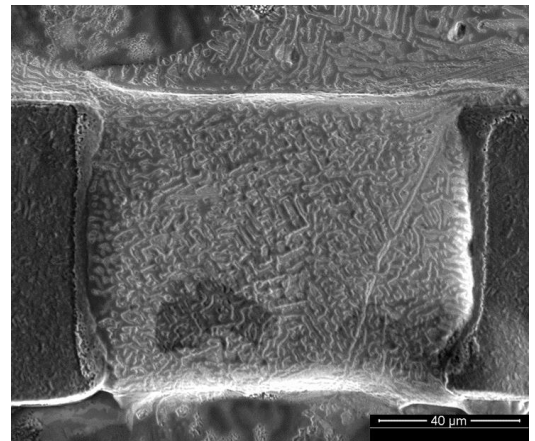


# Fabrication Procedure



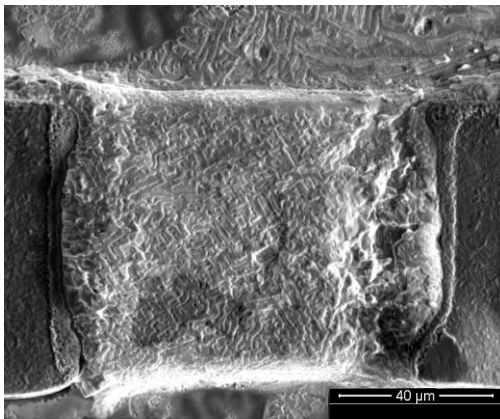
- Use of solder paste allows characterization of any commercially available alloy.
- High temperature photoresist (AZ 15 nXT) enables reflow with solder mask on.

# Electromigration Testing

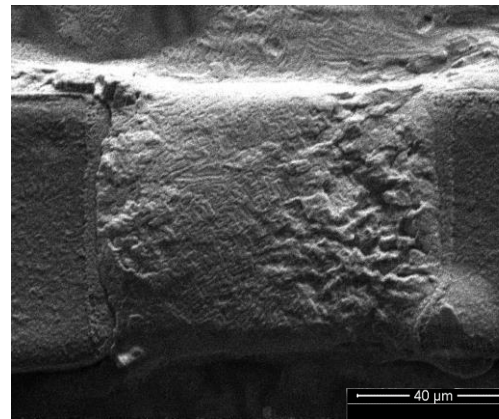


SEM  
Images

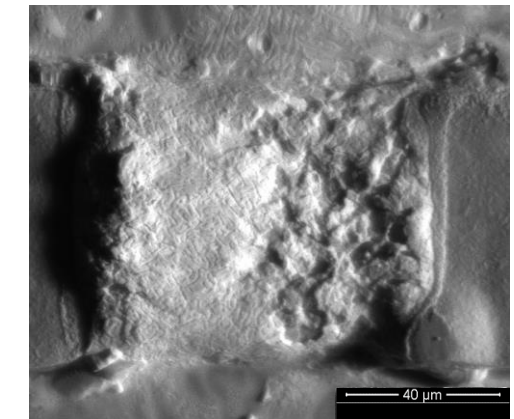
105 °C  
62.5 kA/cm<sup>2</sup>



3 hr



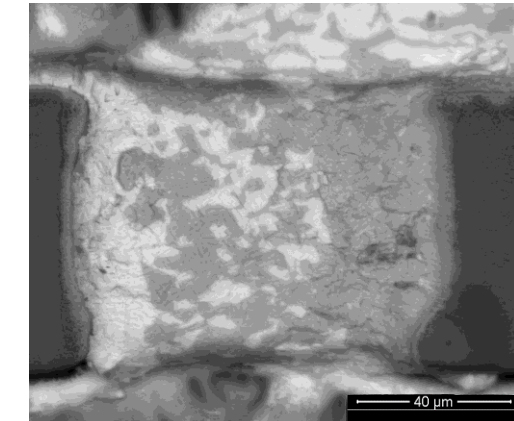
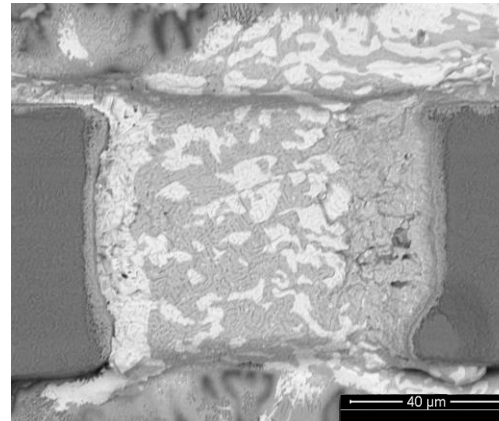
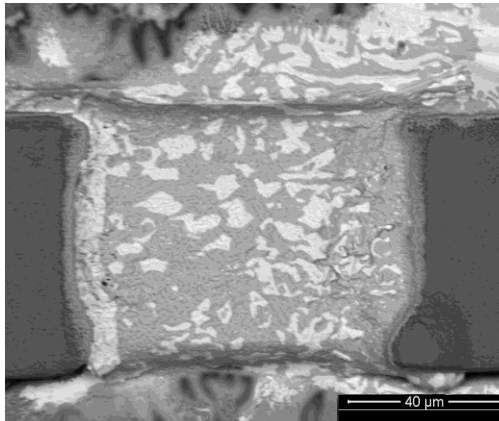
9 hr



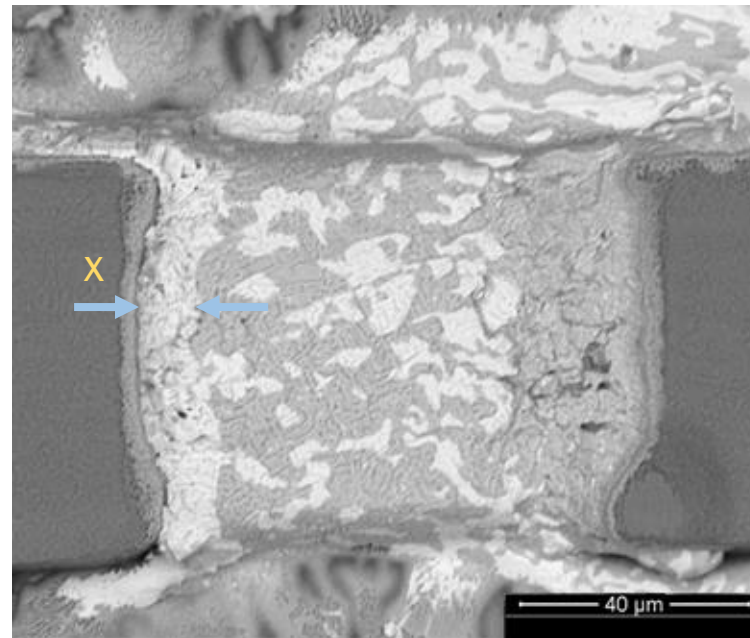
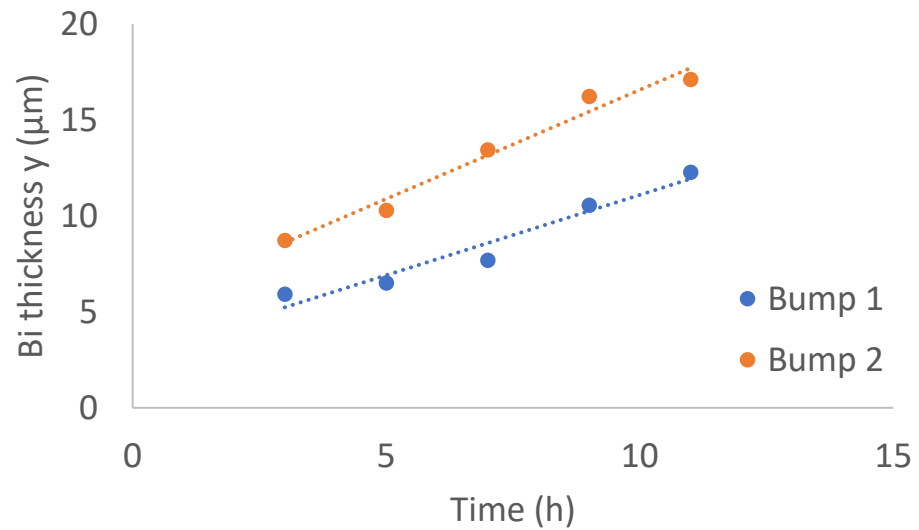
15 hr

Bi phase accumulation visible  
under BSED Images

BSE  
Images



# Bi Thickness Measurement



105 °C  
 $6.25 \times 10^4 \text{ A/cm}^2$

- Thickness measured at 10 points and averaged
- Shows linear variation with time

# Calculation of Diffusivity

$$J_{Bi} = \frac{CD}{kT} Z^* e\rho j \quad \rightarrow \quad DZ^* = J_{Bi} C \frac{kT}{e\rho j}$$

$J_{Bi}$ : Flux of Bi

$C$ : Concentration of Bi

$D$ : Diffusivity of Bi

$Z^*$ : Effective Valence

How to get  $J_{Bi}$  from experiments?

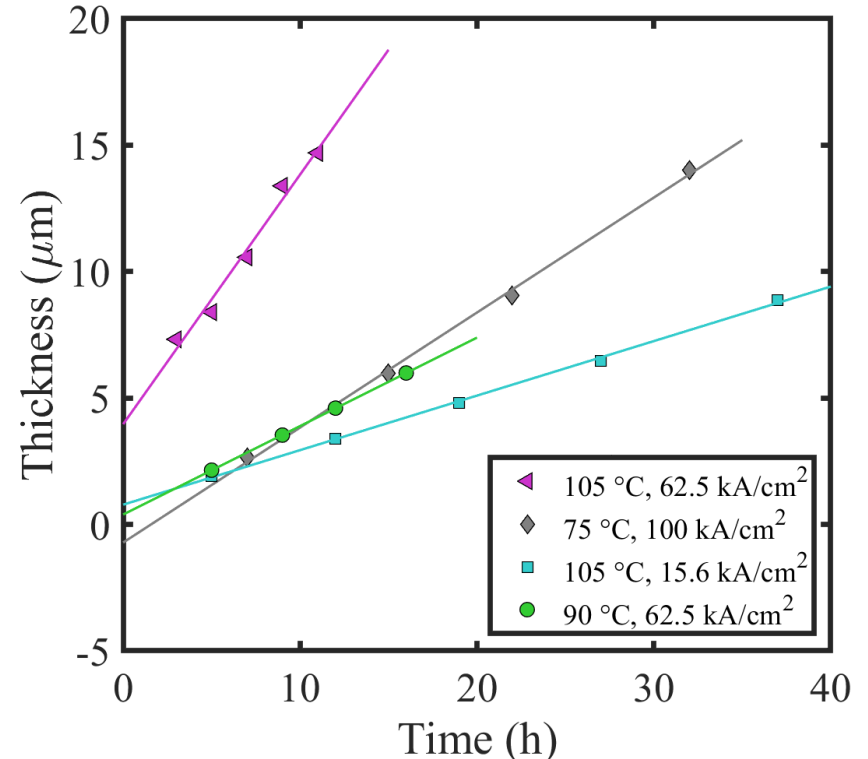
$$J_{Bi} = \frac{dx}{dt} \times d \times \frac{N}{m} \times 0.43$$

Atoms per m<sup>3</sup>

57% of the Bi was already present in the eutectic, only 43% had to move to make it Bi phase

Rate of Bi growth from experiments

L.-T. Chen and C.-M. Chen, (2006)

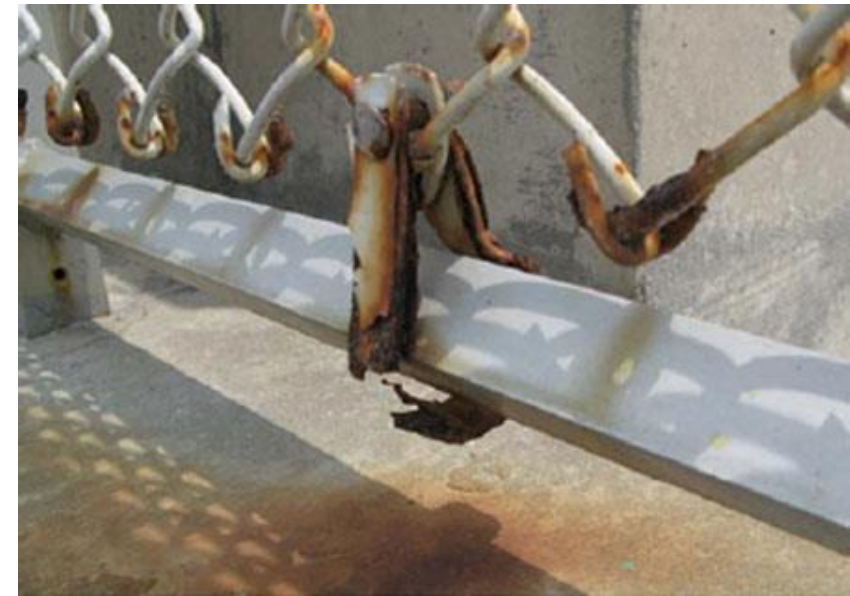


Average thickness variation with time

# Other Failures

# Corrosion

- Result of oxidation
  - Very common in nature (pure forms of metal difficult to find)
- Three types: dry, wet, or humidity-induced
- Dry oxidation converts metal into oxide
  - Occurs at relatively high temperatures
- Wet oxidation form metal hydroxides
  - Occurs at relatively low temperatures



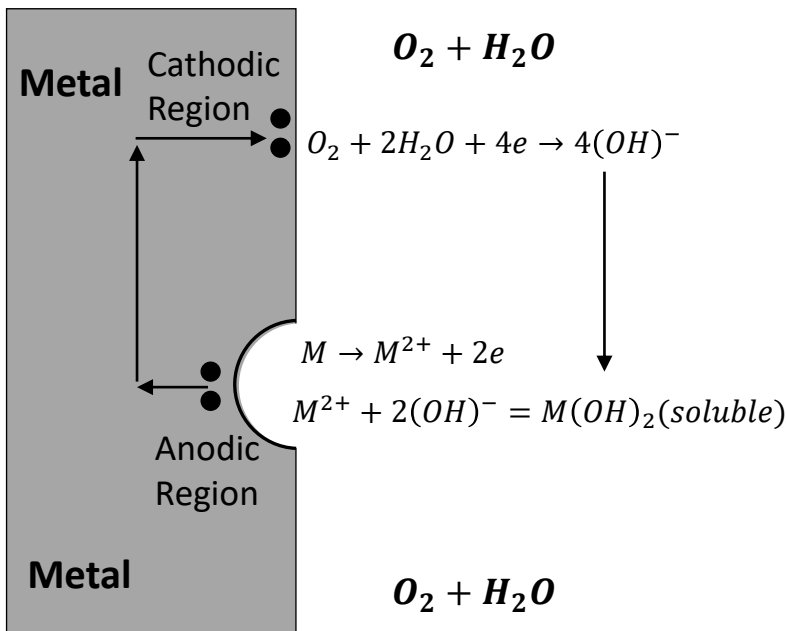
Corrosion failure of a U-type metal support clamp. The metal at the bottom of the support clamp has corroded away. Corrosion rate was greatest in the regions where the metal was severely bent

Source: J.W. McPherson, Reliability Physics and Engineering: Time to Failure Modeling, 2<sup>nd</sup> Edition, Springer, 2013.

# Electrolytic (Wet) Corrosion

- Different from dry oxidation
- $M(OH)_n$  form during wet oxidation
- Occurs at low temperature compared to dry oxidation
- Metal hydroxides dissolve in water (exposes new metal to corrosion)
- Corrosion time to failure

$$TF = A_0 \exp\left(\frac{Q}{k_B T}\right)$$



Metal wet-corrosion (corrosion in aerated water) results in metal-hydroxide [ $M_x(OH)_y$ ] formation on the surface of the metal. Metal hydroxides can dissolve in water, thus exposing fresh metal for continued corrosion. Certain regions in the metal can become anodic, relative to other locations, depending on mechanical stress differences, grain size differences, impurity concentration differences, impressed potentials, etc.

Source: J.W. McPherson, Reliability Physics and Engineering: Time to Failure Modeling, 2<sup>nd</sup> Edition, Springer, 2013.

# Standard Electrode Potentials

Metal	Oxidation state	Standard electrode potential: $V_0$ (Volts)
Mg	$Mg^{2+} + 2e$	-2.36
Al	$Al^{3+} + 3e$	-1.66
Zn	$Zn^{2+} + 2e$	-0.76
Cr	$Cr^{3+} + 3e$	-0.74
Fe	$Fe^{2+} + 2e$	-0.44
Cd	$Cd^{2+} + 2e$	-0.40
Co	$Co^{2+} + 2e$	-0.28
Ni	$Ni^{2+} + 2e$	-0.25
Sn	$Sn^{2+} + 2e$	-0.14
Pb	$Pb^{2+} + 2e$	-0.13
H <sub>2</sub>	$2H^{+} + 2e$	0
Cu	$Cu^{2+} + 2e$	0.34
Ag	$Ag^{+} + e$	0.8
Pd	$Pd^{2+} + 2e$	0.99
Pt	$Pt^{2+} + 2e$	1.2
Au	$Au^{3+} + 3e$	1.5

More Anodic

Reference Electrode

More Cathodic

Al  
Pt

Platinum-Aluminum pad  
metallization – Corrosion  
risk?

$$\Delta G = (ze)\Delta V_0$$

Source: J.W. McPherson, Reliability Physics and Engineering:  
Time to Failure Modeling, 2<sup>nd</sup> Edition, Springer, 2013.

# Wet Corrosion

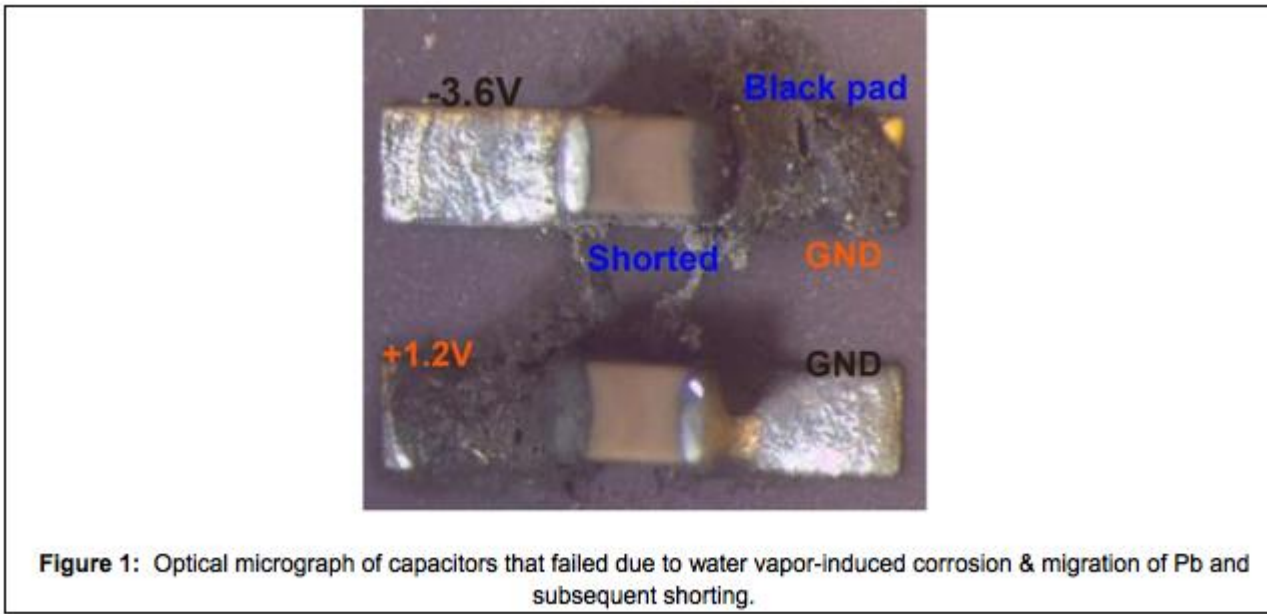


**Figure 1:** Optical micrograph of capacitors that failed due to water vapor-induced corrosion & migration of Pb and subsequent shorting.

<https://www.dfrsolutions.com/moisture-in-hermetic-packages>